Biochimica et Biophysica Acta 1797 (2010) 391–405

Contents lists available at ScienceDirect

Biochimica et Biophysica Acta

journal homepage: www.elsevier.com/locate/bbabio

Chloroplastic oxidative burst induced by tenuazonic acid, a natural photosynthesis inhibitor, triggers cell necrosis in *Eupatorium adenophorum* Spreng

Shiguo Chen, Chunyan Yin, Sheng Qiang *, Fenyan Zhou, Xinbin Dai [1]

Weed Research Laboratory, Nanjing Agricultural University, Nanjing 210095, China

ARTICLE INFO

Article history:
Received 12 August 2009
Received in revised form 8 December 2009
Accepted 14 December 2009
Available online 21 December 2009

Keywords:
TeA
Chloroplast
ROS
Mode of action
Phytotoxin
Photosynthesis inhibitor

ABSTRACT

Tenuazonic acid (TeA), a nonhost-specific phytotoxin produced by *Alternaria alternata*, was determined to be a novel natural photosynthesis inhibitor owning several action sites in chloroplasts. To further elucidate the mode of its action, studies were conducted to assess the production and involvement of reactive oxygen species (ROS) in the toxic activity of TeA. A series of experiments indicated that TeA treatment can induce chloroplast-derived ROS generation including not only $^1O_2$ but also $O_2^{\cdot-}$, H_2O_2 and $^{\cdot}OH$ in *Eupatorium adenophorum* mesophyll cells, resulting from electron leakage and charge recombination in PSII as well as thylakoid overenergization due to inhibition of the PSII electron transport beyond Q_A and the reduction of end acceptors on the PSI acceptor side and chloroplast ATPase activity. The initial production of TeA-induced ROS was restricted to chloroplasts and accompanied with a certain degree of chloroplast damage. Subsequently, abundant ROS were quickly dispersed throughout whole cell and cellular compartments, causing a series of irreversible cellular harm such as chlorophyll breakdown, lipid peroxidation, plasma membrane rupture, chromatin condensation, DNA cleavage, and organelle disintegration, and finally resulting in rapid cell destruction and leaf necrosis. These results show that TeA causing cell necrosis of host-plants is a result of direct oxidative damage from chloroplast-mediated ROS eruption.

1. Introduction

TeA is a nonhost-specific phytotoxin produced by several fungi including *Alternaria alternata*, *A. longipes* and *A. tenuissima* [1]. It causes symptoms of brown leaf-spot disease in a wide range of plants from weed species to crop plants, and then quickly kills the seedlings of mono- and dicotyledonous weeds, especially *Eupatorium adenophorum* (Asteraceae), a noxious weed, that is found throughout the world [2]. Therefore, TeA has a potential to be developed as a new bioherbicide (Supplementary-1). Although it was isolated in 1957 from the culture filtrates of *A. tenuis* [3], so far, interest in TeA was mainly focused on concerns with toxicity [4,5] as well as desirable bioactivity including antitumor, antiviral and antibacterial activity due to inhibiting protein synthesis [6,7]. Conversely, Meazza et al. found that TeA weakly inhibits p-hydroxyphenylpyruvate dioxygenase [8]. Recently, we reported that TeA is a novel photosynthesis inhibitor with several action sites, which mainly interrupts photosystem II (PSII) electron transport beyond Q_A (primary quinone acceptor) by competing with Q_B (secondary quinone acceptor) for Q_B-niche of the D1 protein. Based on studies with D1-mutants of *Chlamydomonas reinhardtii*, the no. 256 amino acid plays a key role in TeA binding to Q_B-niche. Moreover, TeA is the first toxin from a phytopathogen reported as a natural PSII inhibitor [9,10]. However, it is still unknown how TeA induces cell death and causes leaf necrosis.

Under such stresses of pathogen attack and herbicide treatment, reactive oxygen species (ROS) are usually considered to be involved in cell death processes as signal or toxic molecules. In plants, the ROS burst triggered by different stresses are attributed to different mechanisms [11,12]. A large body of investigations have pointed out that plant pathogenic toxins could induce ROS production in mitochondria, plastids and other organelles of the host-plant cell. For example, victorin, a host-selective peptide toxin from *Cochliobolus victoriae*, causes mitochondrial oxidative burst by inhibiting the respiration chain [13]. Fumonisin B1 (FB1), a sphinganine analog mycotoxins produced by *Fusarium moniliforme*, can elicit an apoplastic oxidative burst in *Arabidopsis* by peroxidase [14]. Shinogi et al. showed that AK-toxin I from *A. alternata* triggered ROS generation in plasma membranes of sensitive Japanese pear due to its direct action on plasma membrane [15]. Gechev et al. suggested that a biphasic oxidative burst in *Arabidopsis* leaf tissue following treatment with the host-specific toxin AAL-toxin from *A. alternata* resulted from toxin-induction of genes encoding ROS-generating proteins [16]. During the interaction of these phytotoxins and host-plants, ROS have been shown to be involved in programmed cell death (PCD) pathway. Additionally, there are a few reports that some toxins such as taboxin from *Pseudomonas syringae* pv *tabaci*, naphthazarin toxin produced

* Corresponding author. Tel./fax: +86 25 84395117.
E-mail address: wrl@njau.edu.cn (S. Qiang).
[1] Current address: Plant Biology Division, The Sam Robert Noble Foundation, Ardmore, OK 73401, USA.

0005-2728/$ – see front matter © 2009 Elsevier B.V. All rights reserved.
doi:10.1016/j.bbabio.2009.12.007

by *Fusarium solani* can generate $^1O_2$ and $O_2^{\cdot-}$ in chloroplasts under light due to interruption of PSI electron transport chain [17,18]. To the best of our knowledge, the mechanism of chloroplastic oxidative burst induced by some toxins from plant pathogens is still vague, moreover, no report on chloroplastic oxidative burst triggered by a natural PSII inhibitor toxin has been available.

In plant cells, chloroplasts are considered to be the major site of ROS production, since they possess an environment rich in oxygen, reductants, and high-energy intermediates [11,19]. A complex array of ROS can be generated in choroplasts resulting from the accumulation of $^1O_2$ when the absorption of light energy exceeds the capacity for CO_2 assimilation or leads to inactivation of PSII reaction centers due to overreduction of the electron transport chain [20] and $O_2^{\cdot-}$ due to the photoreduction of oxygen at PSI at high light intensities. Photosynthesis inhibitors are good tools to investigate the mechanism and role of ROS generation in chloroplasts. A large percentage of commercial herbicides are inhibitors of chloroplast electron transport chain. Their primary toxic mechanism is to block the synthesis of ATP and NADPH, being followed by ROS generation, oxidative damage and cell death [21].

Here, we examine the mechanism of ROS generation in mesophyll cells of *E. adenophorum*, oxidative damage, cell death and leaf necrosis phenomena after TeA treatment in order to thoroughly clarify the relationship between the molecular sites of TeA action, ROS and cell necrosis. Through a series of sensitive and robust assays we provide evidence to support the view that TeA-induced chloroplast-derived oxidative burst attributed to the multiple inhibition of photosynthesis causes oxidative damage to cells, resulting in cell death and leaf tissue necrosis. Finally, a model of action of TeA as a natural photosynthesis inhibitor was proposed.

2. Materials and methods

2.1. Plant materials and tenuazonic acid

Cuttings of *E. adenophorum* were rooted and grown in a mixture of soil and peat (1:1 [v/v]) at between 18 to 25 °C under approximate 300 μmol m^{-2} s^{-1} white light (day/night, 12 h/12 h) and relative humidity (about 70%) in a greenhouse. After three months of growth, the second and third top leaves of the plants were used in subsequent experiments.

TeA was isolated and purified from the culture of *A. alternata* isolate 501 [9]. For all experiments, TeA was dissolved in less than 1% methanol (v/v). 5-(Diethoxyphosphoryl)-5-methyl-1-pyrroline-*N*-oxide (DEPMPO) was supplied by Prof. Y. Liu (Institute of Chemistry, CAS). All other chemicals were obtained from Sigma-Aldrich.

2.2. Preparation of leaf segments and treatments

The epidermis was carefully peeled from the abaxial surface of the leaves following the procedure of Yao et al. [22]. The resulting epidermis-less leaf segments of (0.5 × 1 cm) were placed in a small Petri dish containing 10 mM MES-KCl, pH 7.2, in darkness until use. For chemical treatment, leaf segments were transferred to fresh buffer with or without dimethylthiourea (DMTU, 1 mM in 0.2% DMSO), SOD (400 U/ml) and catalase (300 U/ml), then floated on solutions with or without TeA with the peeled surfaces in contact with the liquid and incubated for the time indicated in each experiment under illumination in the growth chamber (25 °C, 100 μmol m^{-2} s^{-1} white light). After washing, samples were used for biochemical and cytological assays.

2.3. Assays of leaf tissue damage and cell viability

To assess lesion formation, detached leaves were vacuum-infiltrated for 15 min with 1% methanol (control) or 250 μM TeA and treated for the indicated times (25 °C, 100 μmol m^{-2} s^{-1} white light). The samples were examined for visible lesions and recorded with a digital camera (Nikon, COOLPIX 4500, Japan). Leaves were stained with Trypan Blue D (TBD) to visualize dead cells in fresh tissue as previously described in detail [23].

2.4. Chlorophyll fluorescence determination

Detached-intact leaves submerged in TeA solution were vacuum-infiltrated for 15 min, continuing to incubate for 3 h at 25 °C in complete darkness. Chlorophyll fluorescence rise kinetics was measured with a HandyPEA fluorometer (Hansatech, UK). The OJIP fluorescence transients are induced by 1 s pulses of red light (650 nm, 3500 μmol m^{-2} s^{-1}). Raw data were transferred with HanyPEA V1.30 software and BiolyzerHP3 to a spreadsheet. The state of PSII reaction center (RC) is characterized on the basis of several JIP-test parameters [24]. Non-Q_A centers are calculated according to the amount of Q_A reducing centers of the reference samples: therefore the fraction in % of non-Q_A reducing centers is equal to 100% minus the fraction of the % of Q_A reducing samples.

2.5. Estimation of chloroplast ATPase activity

Thylakoids were extracted using the method of Jursinic [25]. After thylakoids were treated with TeA at various concentrations for indicated time in ice in dark, thylakoids (40 μg Chl) was added into 1 ml a medium containing 50 mM Tricine-NaOH (pH 8.8), 2.5 mM $MgCl_2$, 5 mM ATP, 20 mM NaCl and 33% (v/v) CH_3OH, and then incubated for 5 min at 37 °C. Mg^{2+}-ATPase activity was determined as hydrolyzed Pi according to [26].

2.6. Electrolyte leakage and lipid peroxidation

To measure ion leakage [23], leaf discs of 7-mm diameter were prepared and rinsed with distilled water, then 20 pieces of them (about 0.1 g) were submerged in 5 ml of distilled water, 1% methanol, 250 μM TeA solution for the indicated times at 25 °C under around 100 μmol m^{-2} s^{-1} white light with occasional agitation. The conductivity of the wash solution (μS cm^{-1}) was determined using a DDS-12A conductivity meter. The total ion leakage was obtained by measuring the conductivity of the same leaf discs-containing solution after autoclaving. Ion leakage per gram of wet weight was calculated by dividing the conductivity of the solution before autoclaving by the conductivity of the solution after autoclaving and dividing the value by sample weight. Relative ion leakage is the ratio of the value obtained in treated samples to the value obtained in samples from control (water) samples.

The level of lipid peroxidation was monitored by spectrophotometric determination of malondialdehyde (MDA) using thiobarbituric acid (TBA) according to Shimizu et al. [27]. The concentration of MDA-reactive TBA was calculated from the extinction coefficient of 155 mM^{-1} cm^{-1}.

2.7. Histochemical detection of H_2O_2 and $O_2^{\cdot-}$

H_2O_2 and $O_2^{\cdot-}$ levels were determined by in vivo staining with 3,3′-diaminobenzidine (DAB) [28] or nitroblue tetrazolium (NBT) [29] as substrate. Briefly, plants were excised at the base stems and supplied through the cut stems with a 0.1% (w/v) solution of DAB (pH 3.8) or 0.1% (w/v) NBT (dissolved in 25 mM HEPES-KOH) for 8 h under light at 25 °C, and then exposed to TeA. The second leaves were cut and rinsed by distilled water, and decolorized by immersing the leaves in boiling ethanol (96%) for 10 min. The latter samples were stored in ethanol (96%) and recorded with a digital camera (Nikon, COOLPIX 4500, Japan). H_2O_2 and $O_2^{\cdot-}$ were visualized as a reddish-brown and dark-blue coloration.

2.8. Laser-scanning confocal microscope (LSCM) observation

Intracellular ROS were measured by monitoring DCF fluorescence, the oxidation product of H_2DCF-DA [30]. Microscopy observation was performed using a LSCM (Leica TCS-SPII, Germany).

For epidermis-less leaf segments, after exposure to experimental treatments, the samples were incubated with 10 μM H_2DCF-DA for 25 min at 37 °C in darkness. After washing with loading buffer (10 mM Tris–HCl, 50 mM KCl, pH 7.2), the samples were examination using 488 nm excitation by 25% power and 510–560 nm emission.

Mesophyll protoplasts were isolated using 1% Cellulase R10 and 0.2% Macerozyme R10 (Yakult Honsha, Tokyo, Japan) according to [31]. Protoplasts were incubated in 10 μM H_2DCF-DA in W5 solution for 15 min at 37 °C in darkness, and washed twice with W5 solution. When TeA was added to H_2DCF-DA preloaded protoplasts, LSCM observation was immediately performed with the following settings: 5% power, 488 nm excitation, and 510–560 nm emission. Fluorescence images were captured over a 10 min period.

Chloroplast autofluorescence (488 nm excitation, 45% power) was visualized at 725–795 nm. Analysis of quantitative images was performed using Leica Confocal Software Lite (Leica, Germany).

2.9. Electron spin resonance (EPR) analysis

PSII membranes were isolated according to the method of Berthold et al. [32]. For EPR analysis [33], PSII membranes (200 μg Chl ml^{-1}) were suspended in 1 mM DM, 2 mM DETAPAC (diethylenetriaminepentaacetic acid), 50 mM MES-NaOH (pH 6.0), 5 mM NaCl, 250 μM TeA and 40 mM DEPMPO as spin trap of $O_2^{\cdot-}$ and ·OH. EPR signals of samples were measured before and after exposure to light with a Bruker ESP300 spectrometer (Bruker Company, Germany) operating in the X-band at 20 °C. Samples were illuminated by a continuous He–

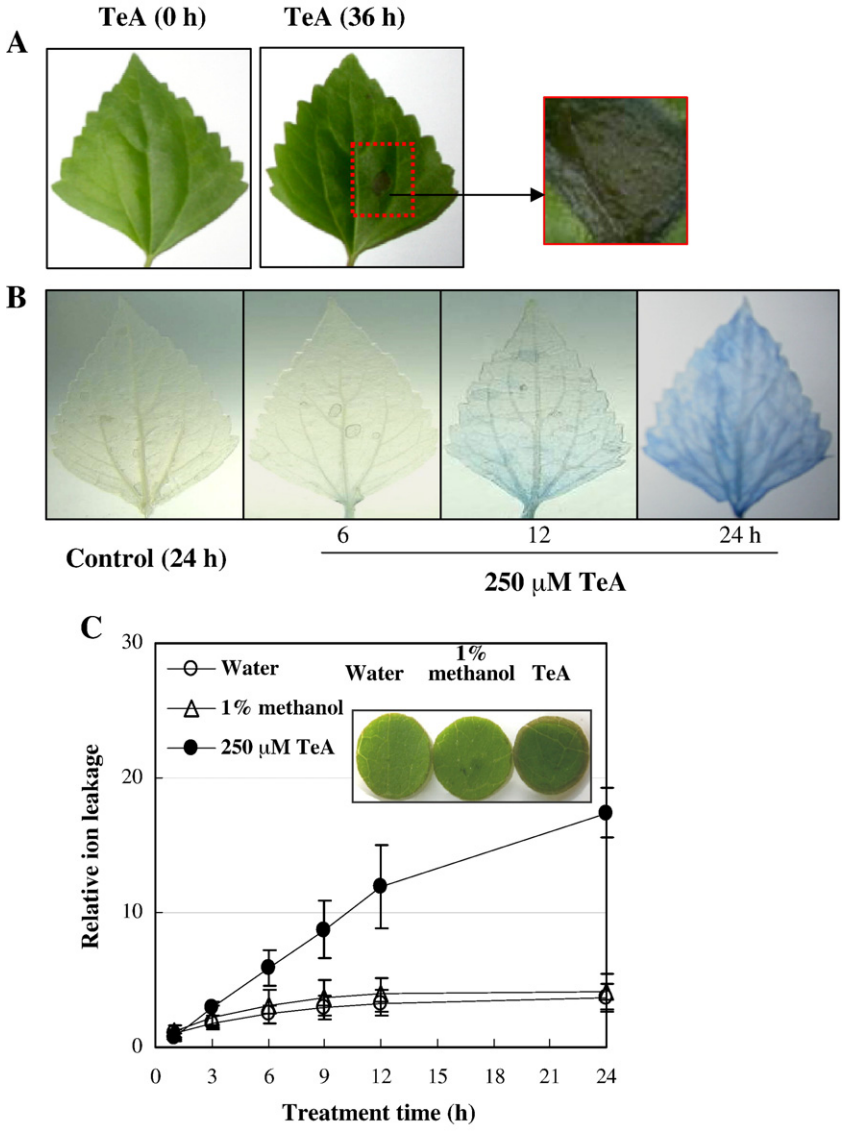

Fig. 1. Detached leaves of *E. adenophorum* responses to TeA. (A) Photographs of detached leaves incubated by 250 μM TeA for 0 and 36 h under illumination (25 °C, 100 μmol m^{-2} s^{-1} white light). Red pane indicates leaf lesions showing a brown diseased leaf-spot. (B) Cell death at 6, 12 and 24 h after 250 μM TeA treatment under light. Leaves were stained with Trypan Blue D. (C) Ion leakage was assayed after leaf discs were treated with 250 μM TeA for 1, 3, 6, 9, 12 and 24 h under illumination. Ion leakage is reported as the ratio of the value measured in 1% methanol or TeA-treated samples to the value obtained in water-treated samples (control) at 1 h; raw value of water-treated samples at 1 h is 84.01 ± 21.35 μS cm^{-1}. Data are presented as means ± SD ($n = 4$). Arrow indicates the time at which cell death was visible. Insert stands for photography of leaves discs incubated for 12 h.

Ne laser (663 nm, 1800 μmol m^{-2} s^{-1}) that produced strong irradiance without heating them. The instrument setting used were as follows: modulation amplitude, 1.5 G; time constant, 164 ms; modulation frequency, 100 kHz; microwave power, 10 mW; and microwave frequency, 9.76 GHz. Detection of $^1O_2$ was carried out with 20 mM 2,2,6,6-tetramethyl-piperidine (TEMP) as spin trap under the same conditions as described above. As described by [34], PSII membranes were extracted into ethylacetate and aired in the presence of catalytic amount PbO_2 before EPR detection in order to avoid artifacts resulting from the production of diamagnetic hydroxylamines. Purification of TEMP was performed by a standard vacuum distillation at 15 mbar in the presence of active carbon.

2.10. Tansmission electron microscope (TEM) procedures

H_2O_2 was visualized at the subcellular level using $CeCl_3$ for localization [35]. Electron-dense cerium deposits that formed in the presence of H_2O_2 were visualized by TEM. TeA-treated epidermis-less leaf segments were cut into small tissue pieces (1–2 mm^2) and incubated in freshly prepared 5 mM $CeCl_3$ in 50 mM 3-(*N*-morpholino) propanesulfonic acid (Mops) at pH 7.2 for 1 h. Tissue pieces were then fixed in 1.25% (v/v) glutaradehyde/1.25% (v/v) paraformaldehyde in 50 mM sodium cacodylate (CAB) buffer, pH 7.2 for 1 h, and held overnight at 4 °C. For the experiments in Fig. 9, segments were not stained in $CeCl_3$ but fixed directly. After fixation, tissues were washed twice for 10 min in CAB buffer and postfixed for 45 min in 1% (v/v) osmium tetroxide, dehydrated in a graded ethanol series (30–100%, v/v), and embedded in Eponaraldite (Agar Aids, Bishop's UK). After 12 h in pure resin, followed by a change of fresh resin for 4 h, samples were polymerized at 60 °C for 48 h. Blocks were sectioned (70–90 nm) on a Power Tome XL microtome (RMC, USA), and mounted on uncoated copper grids (300 mesh). Sections were examined using TEM (H-7650, Hitachi, Japan) at an accelerating voltage of 75 kV.

2.11. Nuclear chromatin condensation and DNA fragmentation analysis

Morphological changes in the nuclear chromatin were detected by staining with 0.5 μg ml^{-1} Hoechst 33258, and followed by observation using a fluorescence microscope (Zeiss Axio Imager A1, Germany) with an excitation filter of 365 nm and a barrier filter of 450 nm.

The DNA degradation assay was performed according to the method of Wang et al. [36]. Identical amounts of DNA sample were run on a 2% (w/v) agarose gel at 80 V. DNA ladders were photographed with an image Saver (Gel DOC™ XR, Bio-Rad, USA).

2.12. Statistical analysis

Relative results were analyzed with STATGRAPHICS PLUS software Ver.2.1 (Manugistics, Rockville, MD, USA). One-way ANOVA was carried out and means were separated using Duncan's least significant ranges (LSR) at 95%. Each experiment was repeated three times with at least three replications per treatment.

3. Results

3.1. TeA-triggered cell death is associated with photosynthesis inhibition

Generally, in the case of detached-intact leaves treated with 250 μM TeA under illumination, visible symptoms began to appear at 24 h, with the tissue turning brown and with spreading collapsed areas, eventually progressing to dry lesions with distinct borders by 36 h (Fig. 1A). The basic timing and sequence of damage formation in TeA-incubated leaves was also monitored by vital dye staining with Trypan Blue or by ion leakage, an indicator of plasma membrane damage (Fig. 1B,C). After TeA incubation for 6 h, ion leakage started to increase but the cells were still alive. Ion leakage enhanced significantly after 12 h, at which time, a portion of the cells began to die. Within 24 h, almost all the cells were dead and ion leakage was also increased to a higher level. Leaf discs edges became brown after 6 h (Supplementary-2), with browning and necrosis progressing toward the center of leaf discs during 12 h of TeA treatment (insert of Fig. 1C). It is clear that occurrence of damage in leaf discs is faster relative to intact leaves. The reason is that TeA infiltrates cells in leaf discs more easily than in intact leaves. Once mesophyll cells contact directly with TeA spray, cell death accompanied by membrane destruction will occur, and soon after leaf tissues will turn brown and necrotic. This pattern seems the same as for leaf injury induced by PSII inhibitor herbicides bentazon and bromoxynil.

The TeA site of action is similar to the classical PSII herbicides including bentazon and bromoxynil, as well as atrazine and diuron, but displays different binding behavior within Q_B-niche on D1 protein [9,10]. To assess the effect of TeA on PSII RCs, we measured chlorophyll fluorescence rise transients of TeA-treated intact leaves (Fig. 2A). The biggest change of fluorescence transients OJIP is a rapid rise of the OJ phase so as to F_J being close to F_M. So, V_J corresponding to the relative variable fluorescence at the J-step showed a distinctly increase, which reflects the accumulation of Q_A^- and rate of Q_A^- reoxidation. Usually, an increase in the J-level is interpreted as evidence for a slowdown of

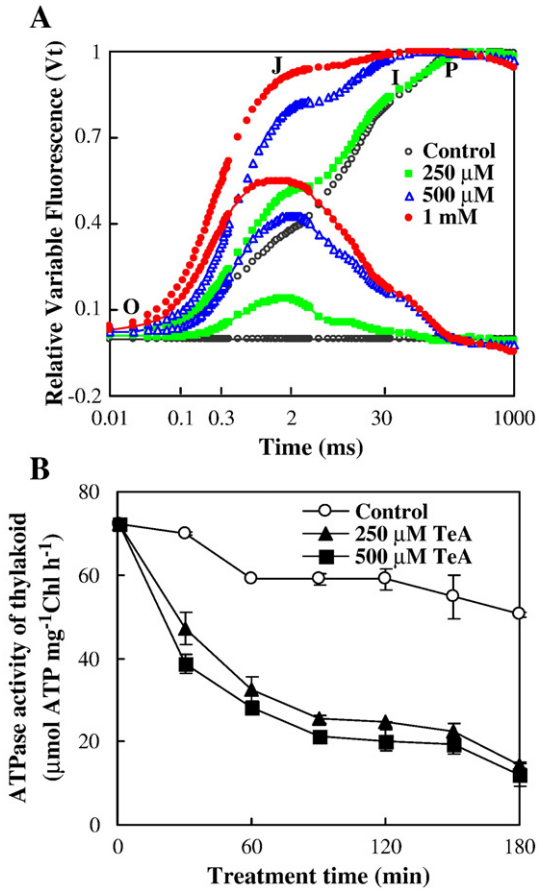

Fig. 2. (A) Chlorophyll fluorescence rise kinetics plotted on logarithmic scale of leaves of *E. adenophorum*. Fluorescence transient OJIP of detached-intact leaves incubated under dark with various concentrations of TeA for 3 h were detected using HandyPEA. The top figures show curves normalized by F_o and F_M, the bottom figures shows delta V (gain 1) full symbol curves minus control. All results are the averages of about 15 independent measurements. (B) Effect of TeA on thylakoid ATPase activity of *E. adenophorum*. After thylakoids were incubated with 1% methanol (control) or TeA for the indicated time in ice under dark, ATPase activity was determined in the presence of Mg^{2+} and ATP, as an increase amount of hydrolyzed Pi. Each value is average of at least three independent experiments.

Table 1
Analysis of Chl fluorescence induction kinetic parameters of TeA-treated leaves of *E. adenophorum*.

	Treatment			
	Control	250 μM TeA	500 μM TeA	1 mM TeA
$V_J = (F_J - F_o) / (F_M - F_o)$	0.40 ± 0.03c	0.55 ± 0.11b	0.59 ± 0.04b	0.75 ± 0.13a
$\Psi_0 = ET_0 / TR_0 = 1 - V_J$	0.60 ± 0.03a	0.45 ± 0.11b	0.41 ± 0.04b	0.25 ± 0.13c
$\varphi_{Eo} = ET_0 / ABS = (1 - F_o / F_M) \cdot (1 - V_J)$	0.47 ± 0.03a	0.34 ± 0.08b	0.20 ± 0.03c	0.09 ± 0.06d
$R_J = (\Psi_{Control} - \Psi_{Treatment}) / \Psi_{Control}\ 1 - \Psi' / \Psi_0$	0d	0.24 ± 0.19c	0.32 ± 0.06b	0.55 ± 0.11a
$N = S_m \cdot M_0 / V_J$	32.70 ± 1.57a	21.75 ± 9.23b	24.61 ± 4.18b	3.32 ± 1.02c
$S_m / t_{Fmax} = [Q_A / Q_{A(total)}]av$	0.06 ± 0.01a	0.03 ± 0.01b	0.02 ± 0.01b	0.01 ± 0.01c
Non-Q_A reducing center	0 ± 0.23d	0.32 ± 0.20c	0.49 ± 0.23b	0.83 ± 0.16a
$\varphi_{Ro} = 1 - F_I / F_M$	0.14 ± 0.01a	0.09 ± 0.01b	0.07 ± 0.02c	0.03 ± 0.04d

Fluorescence parameters in table were measured using HandyPEA after detached-intact leaves were incubated for 3 h in the presence of TeA. Their values are obtained according to the equations of the JIP-test parameters by BiolyzerHP3 program. ABS, TR_0 and ET_0 means absorption, trapping and electron transport flux. Minimal (at 10 μs) and maximal fluorescence is defined as F_o and F_M, respectively; fluorescence intensity at 2 ms (J-step) and 30 ms (I-step) is denoted as F_J and F_I; t_{Fmax} is time to reach F_M; S_m expresses normalised total complementary area above the OJIP transient. Each data is mean values ± SE of 15 repetitions. Different small letters indicate values significantly different within treatments ($p<0.05$) according to the LSR test.

electron flow beyond Q_A [24]. Since PSII electron flow was blocked, the probability ψ_0 that a trapped exciton moves an electron into the electron transport chain beyond Q_A and subsequently, φ_{Eo} which expresses the maximum quantum yield for electron transport, had a sharp decline. When the Q_A^- cannot be reoxidated in time, the turnover number N declined fast, which expresses how many times Q_A has been reduced in the time interval from 0 to t_{Fmax}. The ratio S_m/t_{Fmax} offers a measure of the average (av) redox state of Q_A^-/Q_A from time 0 to t_{Fmax}, and

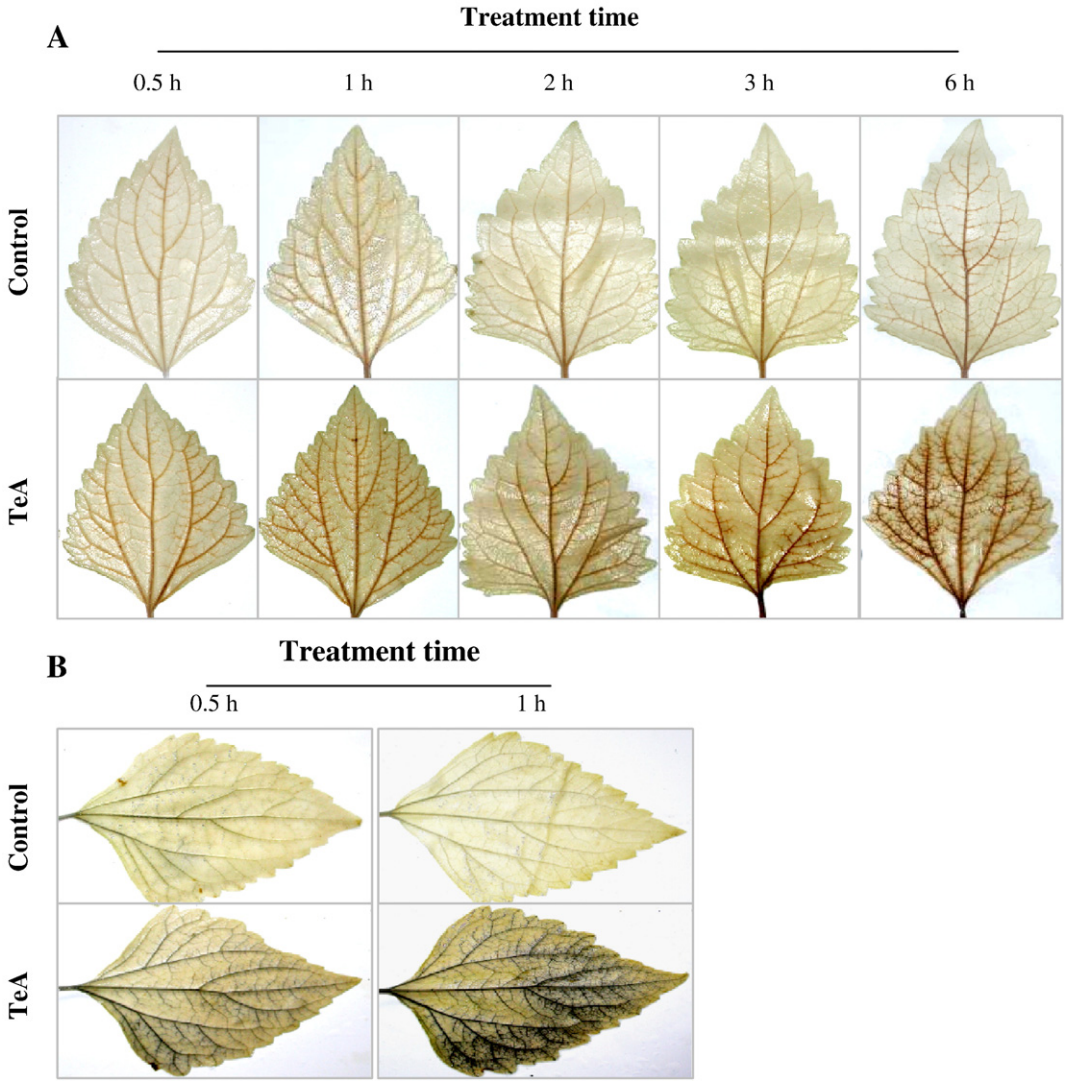

Fig. 3. Histochemical detection of H_2O_2 with DAB staining and O_2^- with NBT staining in the detached-intact leaves of *E. adenophorum*. (A) The induction of H_2O_2 production by 1% methanol (control) or 250 μM TeA for 0.5, 1, 2, 3 and 6 h under illumination (25 °C, 100 μmol m^{-2} s^{-1} white light), respectively. (B) The induction of O_2^- production by 1% methanol (control) or 250 μM TeA for 0.5 and 1 h under light, respectively. Experiments were repeated at least four times with similar results.

expresses also the average fraction of open RCs. A significant decrease of S_m/t_{Fmax} proposed that TeA caused the severe closure of PSII RCs, which can be attributed to an enhancing of the R_J parameter reflecting the number of PSII RCs with Q_B-site filled by TeA. Previous studies suggested that PSII inhibitors can cause an increase of non-Q_A reducing centers [24]. A same change trend of non-Q_A reducing centers is shown in Table 1 after TeA treatment. It is concluded that TeA resulted in inactivation of PSII RCs by blocking electron transport from Q_A to Q_B by occupying Q_B-niche [37,38]. Non-Q_A reducing centers, also so-called heat sink centers or silent centers, are radiators and often are used to protect the system from over excitation and over reduction which would create dangerous ROS. Additionally, TeA treatment had shown an effect on the IP phase (Fig. 2A), which is related to electron transfer through PSI and the reduction of a traffic jam of electrons caused by a transient block at the acceptor side of PSI due to the inactivation of ferredoxin-$NADP^+$-reductase (FNR) [39]. A significant drop of the values of φ_{R0} expressing the probability of reductions at the PSI electron acceptor side per electron flow further than Q_A was found (Table 1), indicating that TeA has a visible effect on electron flow at PSI acceptor side.

The photosynthetic electron transport is coupled to a buildup of a thylakoid proton gradient, which drives the synthesis of ATP from ADP and Pi catalyzed by the chloroplast ATPase [40]. Fig. 2B shows TeA addition inhibited prominently the activity of chloroplast ATPase in the dark. Inhibition of ATPase activity will inevitably lead to blocking ATP synthesis and ATP-hydrolysis. Precisely because TeA interrupts PSII electron flow and ATP synthesis, it is regarded as an inhibitor of redox energy conservation and therefore also is expected to increase the energization levels in thylakoid, which can result in a large generation of ROS. Therefore, it is concluded that TeA-triggered cell death and leaf tissues necrosis may result from oxidative damage due to ROS production by using electrons and the energy of excited photosynthetic units.

3.2. TeA treatment causes oxidative burst before cell death

To monitor weather ROS are involved in the process of TeA-induced cell death, DAB and NBT staining were utilized to check the in situ accumulation of H_2O_2 and O_2^- in detached-intact leaves exposed to TeA under light. H_2O_2 was detectable as early as 0.5 h in TeA-treated leaves,

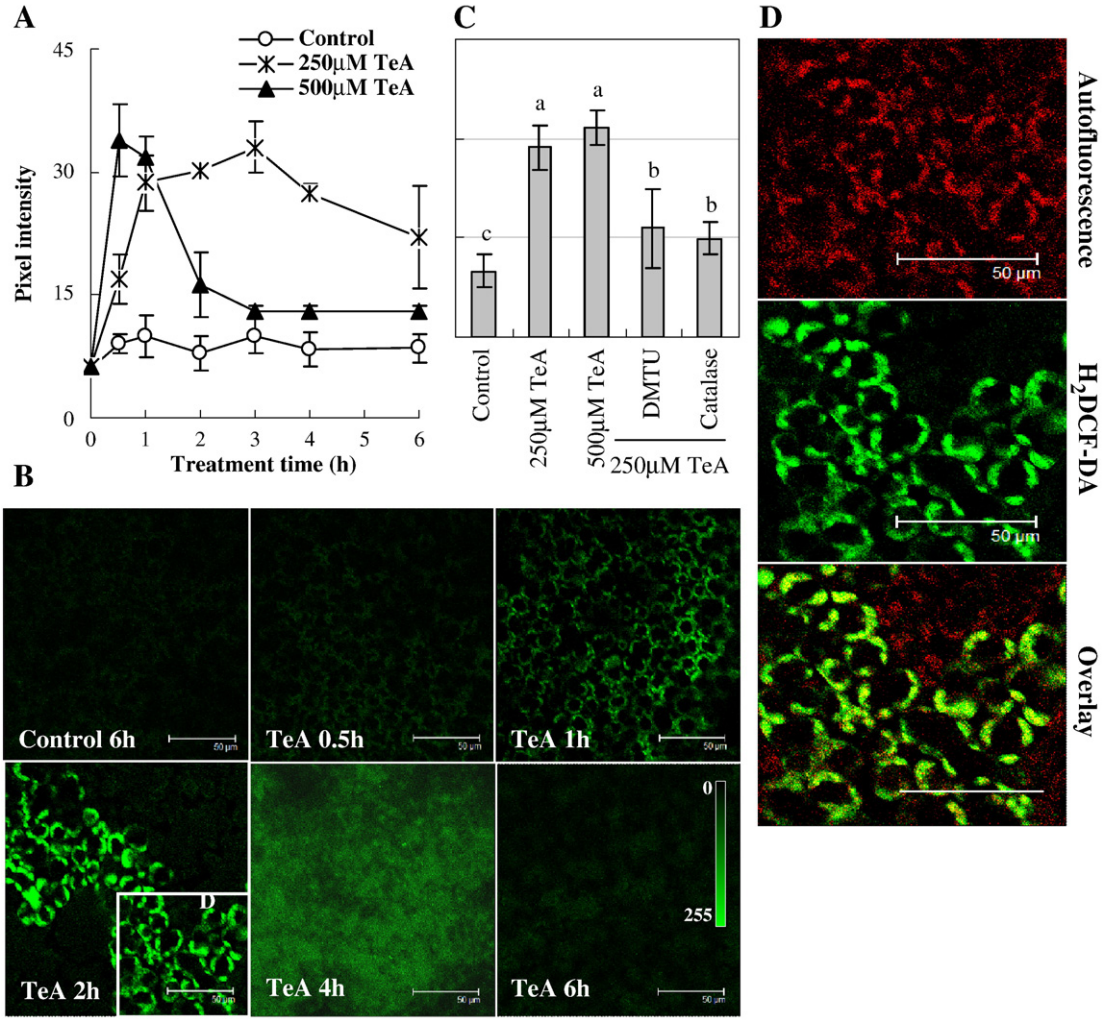

Fig. 4. Production and intracellular localization of ROS in mesophyll cells in epidermis-less leaf segment of *E. adenophorum* after TeA treatment. (A) Time course of change in pixel intensities from images of 1% methanol (control) and TeA-treated mesophyll cells illuminated. (B) DCF fluorescence images of control or 250 μM TeA-treated mesophyll cells at the indicated times. (C) Effect of ROS scavengers on TeA-induced ROS production in mesophyll cells. Mesophyll cells were pretreated with either DMTU (1 mM) or catalase (300 U/ml) for 3 h, subsequently incubated with 250 μM TeA for 4 h under illumination. Data are presented as means ± SD ($n = 3$). Means denoted by the same letter did not significantly differ at $p<0.05$. (D) Mesophyll cells were treated with 250 μM TeA for 2 h. Green signals indicate DCF fluorescence. Red signals indicate chloroplast autofluorescence. Note that the localization of the green fluorescence (DCF) signals matched that of the red fluorescence (autofluorescence) signals. Green signals were not found in the outer membrane of chloroplasts. Bar = 50 μm.

with the color continuing to deepen with incubation over a 6 h period. The color initially appeared in major veins and then spread to minor veins throughout the leaf. However, no visible H_2O_2 accumulation was observed in controls (Fig. 3A). Similar results were observed during detection of $O_2^{\cdot-}$ generation in leaves (Fig. 3B). Incubation of TeA for 0.5 h led to slight accumulation of $O_2^{\cdot-}$ in the vascular tissue. The color was the deepest in intact leaves incubated for 1 h, and then declining. It is presumed that development of H_2O_2 and $O_2^{\cdot-}$ in intact leaves is an earlier event than TeA-induced cell death and leaf necrosis.

3.3. Photosynthetic apparatus of chloroplast is the primary source of TeA-induced oxidative burst

In order to visualize intracellular oxidative processes, the chemical probe H_2DCF-DA combined LSCM was used to monitor ROS generation in epidermis-less leaf segments and protoplasts under light. After segments were treated with 250 or 500 μM TeA (Fig. 4A,B), it appeared that the higher TeA concentration led to an earlier ROS production peak in mesophyll cells. Relative to control, cells incubated with 250 μM TeA have higher DCF fluorescence intensity up to 3 h, and then show a gradual disappearance during 3 to 6 h. It is noticeable that DCF signal appeared mainly to be localized in cellular compartments from 0.5 to 2 h. However, DCF signals dramatically increased and were dispersed throughout the cell when mesophyll cells were incubated with TeA for 3 (not shown) or 4 h (Fig. 4B). At this time, intracellular ROS levels appeared to be much higher than that detected with the DCF signals because of a concomitant enhancement in cellular dysfunction leading to leakage of intracellular ROS into extracellular spaces. ROS scavenger DMTU and catalase could partially reduce DCF signals (Fig. 4C). In an attempt to identify the source of ROS at these time points, the chloroplast autofluorescence (red) of mesophyll cells treated with 250 μM TeA for 2 h was synchronized with DCF fluorescence (green). The green DCF signals exactly matched that of the red chloroplast autofluorescence signals, showing a single yellow image when the red chloroplast fluorescence was overlaid with the green DCF signals (Fig. 4D). A similar result also is found in TeA-treated epidermal peels (Supplementary-3). In the early stage of TeA treatment, DCF signals were not observed in the basic epidermal cells (which do not possess chloroplasts) unless those cells were guard cells of stomata, which makes us deduce that TeA-induced ROS was generated only in chloroplast because only the guard cells contain well-developed chloroplasts in normal leaf epidermis [41].

To confirm next that ROS were initially produced in chloroplasts, the process of ROS production in protoplasts incubated by TeA was monitored. Within 30 seconds, protoplasts exhibited distinct DCF signals, which intensified over a period of 10 min. At this juncture, we also found that the intracellular localization of DCF signals accurately matched that of chloroplasts autofluorescence (Fig. 5). This result

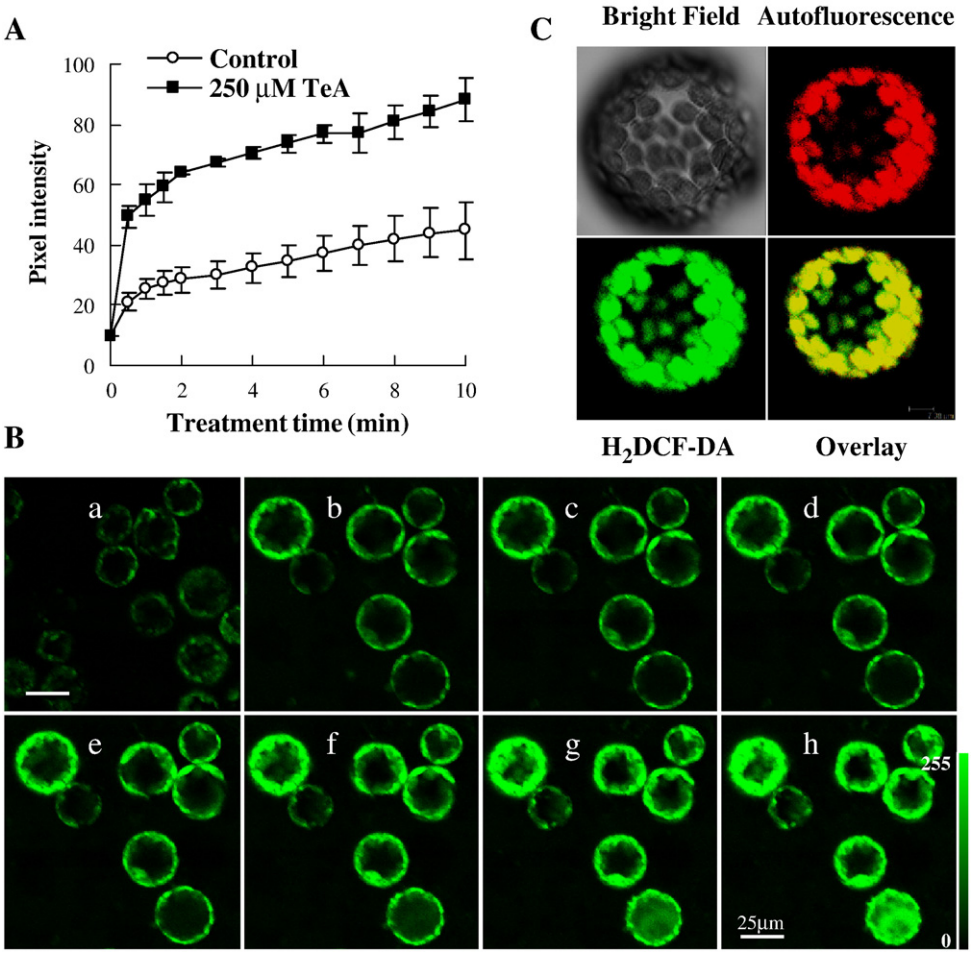

Fig. 5. Production and intracellular localization of ROS in TeA-treated protoplasts of *E. adenophorum*. (A) Time course of changes in pixel intensity determined from images of control or TeA-treated protoplasts. Each data point represents the mean ± SD of three independent experiments in which one value is the means of 7 to 10 individual protoplasts. (B) DCF fluorescence images of control (a, 10 min) or TeA-treated protoplasts (b–h) at different time 0.5 (b), 1 (c), 2 (d), 4 (e), 6 (f), 8 (g) and 10 (h) min. (C) Intracellular localization of ROS after treatment with 250 μM TeA for 10 min. Green signals indicate GFP of DCF. Red signals indicate chloroplast autofluorescence. Note that the localization of the green fluorescence (DCF) signals matched that of the red fluorescence (autofluorescence) signals. Green signals were not found in the outer membrane of chloroplasts.

demonstrates again that the sites of ROS-producing organelles are chloroplasts in TeA-treated cells.

For a more precise localization of H_2O_2 production in mesophyll cells, we did an unltrastructural analysis using a cytochemical assay based on $CeCl_3$ staining [35]. At 1 h of illuminated TeA-treated leaf segments, abundant deposits of cerium was found in chloroplast grana lamellae and stroma, and along chloroplast membranes (Fig. 6B). Similar results were obtained when segments were treated with 10 μM paraquat for 2 h (Supplementary-4). By 4 h (Fig. 6C), the large accumulation of H_2O_2 was also observed in the cell walls facing intercellular spaces. At this moment, H_2O_2 accumulation in chloroplasts increased to a maximum, decreasing thereafter (Supplementary-5). The decline of H_2O_2 in chloroplast grana lamellae, stroma and membranes at this stage coincided with chloroplast grana lamellae disorganization. The H_2O_2 accumulation in cell walls reached its highest level at 6 h (Fig. 6D). However, control cells were completely free of cerium deposits (Fig. 6A). This result provides strong evidence that the original site of TeA-induced H_2O_2 generation is in chloroplasts, which is in agreement with LSCM experimental results. So, we propose that chloroplast-derived oxidative burst is a result of inhibited photosynthesis because TeA inhibits PSII and PSI electron flow and chloroplast ATPase activity.

3.4. TeA-induced not only $^1O_2$ but also $O_2^{\cdot-}$ and $^{\cdot}OH$ generation in PSII

To verify the kinds of ROS generation in chloroplasts, EPR combined spin trap TEMP was used to trap $^1O_2$ formation during PSII membranes incubated with 250 μM TeA. Fig. 7A shows the characteristic EPR signal of nitroxyl radical TEMPO formed by the reaction of TEMP with $^1O_2$. $^1O_2$ was generated by PSII membranes exposed for 15 min to high light illumination. When TeA was added prior to the illumination, the TEMPO signal was around four times the size of that obtained under no light in the presence of TeA or under illumination in the absence of TeA (Fig. 7A). Prolonged illumination resulted in a linear increase of TEMPO signal size in TeA-incubated PSII (Fig. 7B), indicating that TeA caused fast $^1O_2$ generation. Previous studies showed that ROS formation is dominated by $^1O_2$ during PSII acceptor side photoinhibition [34,42]. Some commercial herbicides, such as urea and the phenolics, are known to bind to Q_B-site of PSII. This blocks electron transport and leads to PSII acceptor side photoinhibition, resulting in chlorophyll-mediated $^1O_2$ generation and the oxidative damage to photosynthetic organelles [43]. On this point, TeA is similar as the classical photosynthesis herbicides.

Despite the arguments for $^1O_2$ as a main source of PSII, other ROS also can be produced [44]. We simultaneously estimated the production of $O_2^{\cdot-}$ and $^{\cdot}OH$ by spin trap DEPMPO. As shown by EPR signal curves in Fig. 7C, a distinct $O_2^{\cdot-}$ adduct DEPMPO-OOH was yielded in TeA-treated PSII under strong light. The EPR signal size of $O_2^{\cdot-}$ was further increased with increasing illumination time (Fig. 7D). An approximately 67% increase of the amount of $^{\cdot}OH$ adduct DEPMPO-OH was also observed in the presence of TeA under high illumination for 5 min compared with controls without TeA (Fig. 7C,D). This results show that TeA can induce the formation of $O_2^{\cdot-}$ and $^{\cdot}OH$ in illuminated tissues.

3.5. Chloroplast-derived oxidative burst plays a main role in TeA-caused cellular damage

Experimental results from chloroplast autofluorescence (Supplementary-6) and cell viability (Supplementary-7) showed that chloroplast damage has already begun in early stages of TeA-induced cellular ROS burst, which is an earlier event than the loss of cell viability. Based on the observation that ROS scavengers DMTU, SOD and catalase could suppress the damage to chloroplasts and cell viability, it is proposed that chloroplast-generated ROS plays an important role in chloroplast damage and cell membrane destruction

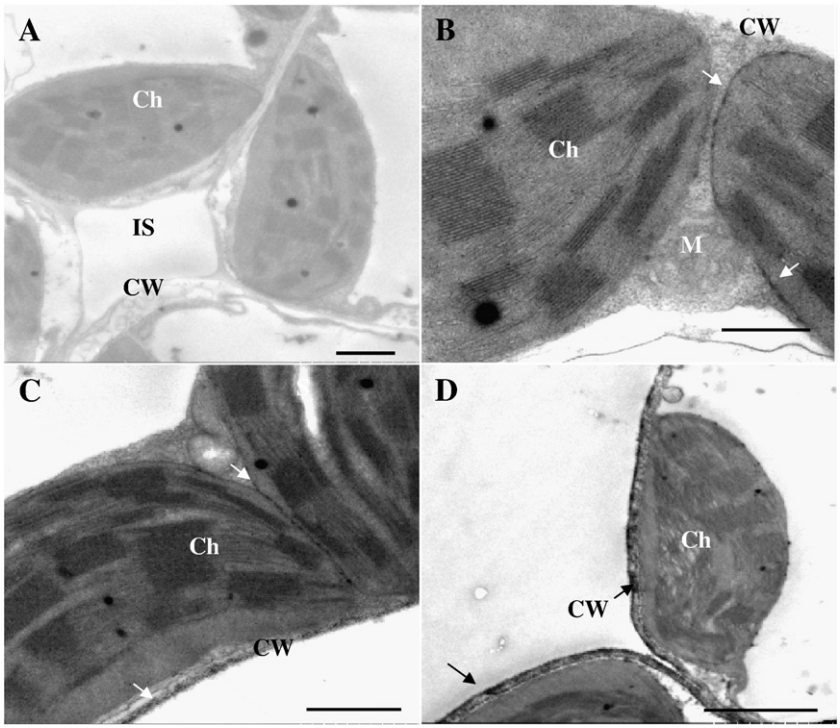

Fig. 6. Cytochemical localization of TeA-inducible H_2O_2 accumulation in mesophyll cells of *E. adenophorum*. Epidermis-less leaf segments were induced with 1% methanol (control) for 6 h or 250 μM TeA for the indicated times under illumination. Experiments were repeated three times with similar results. (A) Control sample had no H_2O_2 accumulation. (B) After 1 h, cerium perhydroxide deposits in the chloroplast membrane (arrows) of mesophyll cells. (C) At 4 h, H_2O_2 production in chloroplast and cell wall (arrows) of mesophyll cells. (D) In mecophyll cells treated with TeA for 6 h, H_2O_2 accumulation in cell wall. Note that chloroplast grana lamellae turned to be distorted. CW, cell wall; Ch, chloroplast; M, mitochondrion; S, starch; IS, intercellular space. (A) Bar = 1 μm; (B–C) bar = 500 nm; (D) bar = 2 μm.

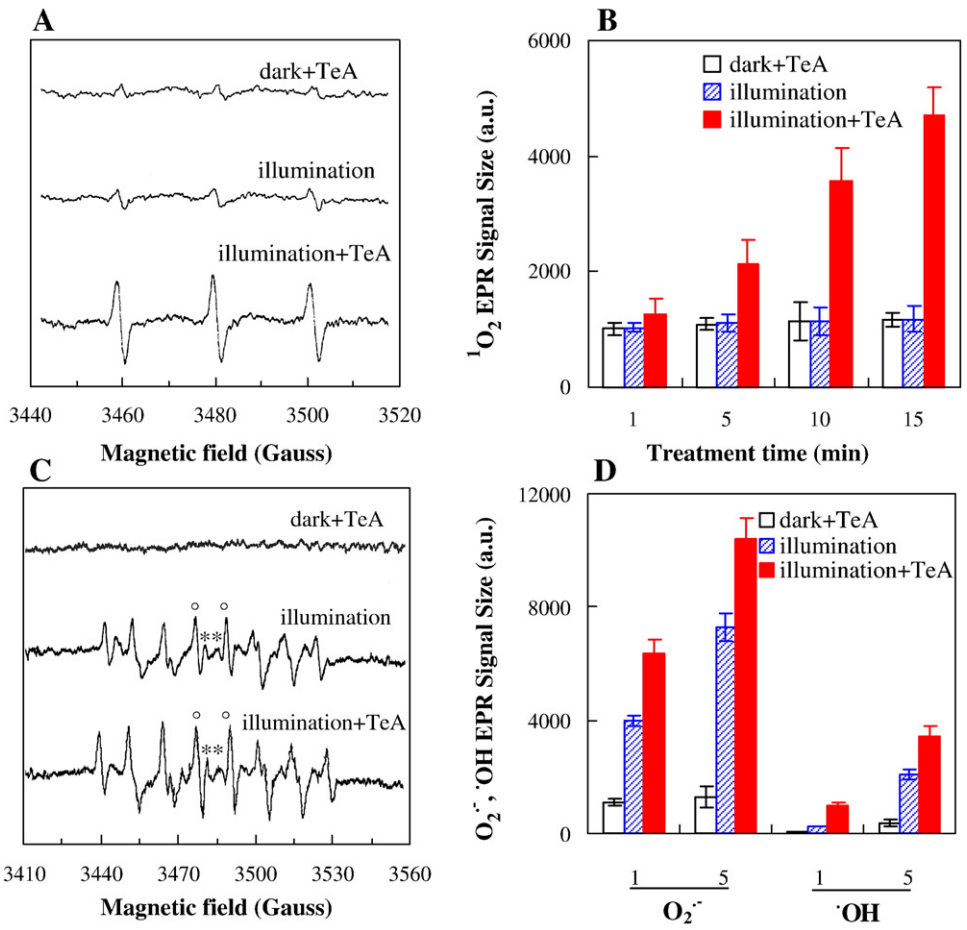

Fig. 7. EPR detection of singlet oxygen ($^1O_2$) trapped by TEMP and free radicals trapped by DEPMPO. (A) Typical EPR spectra of TEMPO as adduct of the reaction of TEMP with $^1O_2$ after a 15 min treatment. (B) Relative intensity of $^1O_2$ EPR signal. (C) Typical EPR spectra of trapped superoxide radicals ($O_2^{\cdot-}$) and hydroxyl radicals (·OH) after a 5 min treatment. (D) Relative intensity of $O_2^{\cdot-}$ and ·OH signal size. PSII membranes of *E. adenophorum* were illuminated with red light (1800 μmol m^{-2} s^{-1}) in the presence of 20 mM TEMP or 40 mM DEPMPO. Circles (°) and asterisks (*) show the characteristic lines corresponding to the $O_2^{\cdot-}$ and ·OH adducts.

during TeA-induced cell death pathway. The loss of cell viability means that TeA treatment destroyed the lipid rich plasma membrane. Furthermore, chloroplasts contain large quantities of lipids in addition to proteins and pigments. These lipids are particularly sensitive to ROS [45]. Pretreatment with DMTU, SOD and catalase could significantly prevent TeA-induced ion leakage and lipid peroxidation in tissues (Fig. 8), revealing chloroplast-derived oxidative burst caused damage to lipids and membrane integrity.

As shown in Fig. 9, ultrastructural changes of TeA-treated illuminated mesophyll cells were monitored. At 4 h, all organelles remained structurally intact, even though cellular ROS have already increased to the highest level before this time point (at 3 h) (Fig. 4). By 5 h, plasmolysis of cells was evident. Up to 6 h, cells exhibited disorganized grana lamellae and distorted shape of chloroplasts. By 9 h, chloroplast grana lamellae showed significant disintegration with envelopes completely disrupted. Also at this time point, some distortion of mitochondria was observed. After 12 h, there was significant degradation to organelles, particularly to chloroplasts which had formed vesicles and distorted and ruptured cytoderm. It is proposed that chloroplasts are the first and most dramatically affected organelles in the process of TeA-induced mesophyll cell death.

3.6. TeA-induced cell death is not PCD

There is compelling evidence that ROS can activate a PCD pathway during plant response to pathogens [46,47]. Typical biochemical hallmarks of PCD in plants include chromatin condensation, DNA ladders, phosphatidylserine exposure, activation of specific proteases, Ca^{2+} influx and cytochrome *c* release [48]. As shown in Fig. 10A–B, a marked increase of the amount of condensed nuclei with high blue fluorescence intensity was seen by an addition of TeA-treatment time. In TeA-incubated samples (250 μM), chromatin condensation had begun by 6 h. However, the event of chromatin condensation does not always mean PCD since a high level of ROS causes direct damage to nucleic acids [49]. Therefore, DNA ladders were analyzed to further test this hypothesis. Electrophoretic analysis revealed that TeA treatment caused varying degrees of DNA fragmentation. However, no visible 180 bp DNA ladders were detected on agarose gels, and only the degradation of some high molecular weight DNA could be observed even after 24 h (Fig. 10D). Interestingly, the addition of DMTU, SOD and catalase can effectively suppress this chromatin condensation (Fig. 10C) and DNA cleavage (Fig. 10D). These results showed that chloroplast-originated oxidative burst indeed led to serious nuclear damage, but did not trigger obvious PCD response during TeA-induced cell death of leaf tissue.

4. Discussion

Our data reveal that TeA treatment resulted in the significant accumulation of H_2O_2 and $O_2^{\cdot-}$ within leaves during leaf necrosis (Figs. 1 and 3). From the analysis of the time of ROS generation and cell death, TeA-induced ROS burst (Fig. 3) is prior to membrane

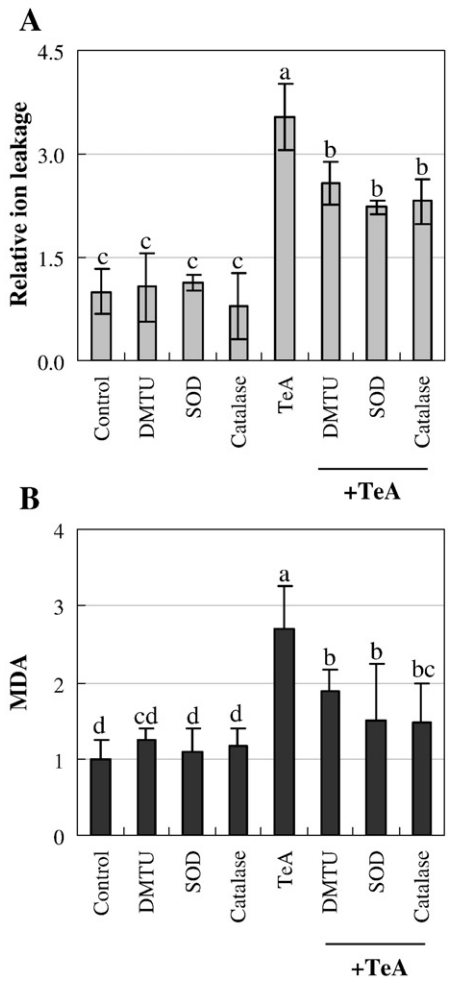

Fig. 8. Effect of ROS scavengers on ion leakage and lipid peroxidation induced by TeA. (A) Effect of ROS scavengers on ion leakage of leaf discs. Leaf discs of *E. adenophorum* were pretreated with DMTU (1 mM) or SOD (400 U/ml) or catalase (300 U/ml) for 3 h, and then exposed to 250 μM TeA for 12 h under illumination. Ion leakage was determined as described in Materials and methods, reported as the ratio of TeA-treated/control value, raw value of control is 177.25 ± 56.44 μS cm^{-1}. (B) Effect of ROS scavengers on lipid peroxidation of mesophyll cells. Epidermis-less leaf segments of *E. adenophorum* were pretreated with DMTU, SOD, catalase for 3 h, and then incubated in 250 μM TeA for 6 h under illumination. Data were calculated as the ratio value of the control sample. The value of control is 2.20 μmol g^{-1} FW. Data are presented as means ± SD ($n = 4$). Means denoted by the same letter did not significantly differ at $p < 0.05$.

damage which is earlier compared with appearance of evident physiological damage attributed to turgor loss and tissue collapse (Fig. 1). It is undoubted that ROS burst plays an important role in the process of TeA-triggered cell death and leaf tissues necrosis.

4.1. Chloroplast-derived oxidative burst is a consequence of inhibition of photosynthesis

Our evidence shows that TeA elicited a fast burst of ROS from chloroplasts, which diffused to outer membrane, cytoplasm, and even intercellular spaces (Figs. 4–6).

In chloroplasts, $^1O_2$ is continuously produced by PSII when photosynthetic electron transport chain was over reduced [11]. Generally, there are three mechanisms for photosynthesis herbicides to produce $^1O_2$ in chloroplasts [18]. Firstly, for herbicides inhibiting carotenoid biosynthesis, they lead to $^1O_2$ production because that excess excited chlorophyll triplet state (^{3}Chl) can no longer be quenched by the production of triplet state β-carotene [50]. Secondly, protoporphyrin IX as a photosensitizer is accumulated and reacts with $^3O_2$ to produce $^1O_2$ when the chlorophyll biosynthetic enzyme PPO is inhibited [51]. For PSII inhibitor herbicides, charge recombination occurring in herbicide-treated PSII can lead to formation of ^{3}Chl and this ^{3}Chl can react with $^3O_2$ to form $^1O_2$ [43,52]. As PSII inhibitor, TeA inhibits electron flow beyond Q_A by binding to Q_B-niche ([9], Table 1), causing a fast accumulation of Q_A^- and ensuing closure of PSII RCs (Fig. 2A, Table 1). Once the forward electron transport cannot proceed, electron back reaction will occur, leading to the leakage of electrons to O_2 and subsequent significant $^1O_2$ formation in PSII illuminated ([43], Fig. 7A,B). For various classes of herbicides with different binding behavior in Q_B-niche, it is different that the charge recombination pathway within PSII RCs where forward electron flow to Q_B is energetically disfavoured. This finally results in a big difference on the yield of $^1O_2$ [43,51,53]. Fufezan et al. demonstrated that the amount of $^1O_2$ in PSII with bromoxynil was twice that than with diuron [42]. This is explained by different charge recombination pathways in the presence of phenolic PSII inhibitors versus urea- or triazine-type PSII inhibitors [53]. Since TeA has a different binding behavior within Q_B-niche from atrazine and diuron [9], the mechanism of TeA-induced $^1O_2$ production in PSII might be different from that of other known PSII inhibitors.

PSII photoinhibitory damage can result in the formation of a complex array of ROS beside $^1O_2$ in chloroplasts [20,42,54]. All results from histochemical (Fig. 3), DCF (Figs. 4 and 5) and cytochemical staining (Fig. 6) showed that TeA treatment caused the generation of large amount of H_2O_2 and $O_2^{\cdot-}$ in chloroplasts because these dyes including DAB, NBT, H_2DCF-DA and $CeCl_3$ are specific molecules used to indicate H_2O_2 and $O_2^{\cdot-}$. EPR evidence also indicated that a clear increase of $O_2^{\cdot-}$ and $^{\cdot}$OH is observed in TeA-treated PSII in the light (Fig. 7C–D). It is suggested that the reduction of O_2 is the starting point for a series of reactions leading to ROS generation on the PSII electron acceptor side [55]. $O_2^{\cdot-}$ are generated by PSII via electron transport to O_2 under reducing conditions. Evidence has been provided that $Pheo^-$ and Q_A^- and Cyt b_{559} [42,44,55,56] and Q_B [57] can serve as the reductant of O_2. Further reduction of $O_2^{\cdot-}$ within PSII will produce other two ROS such as H_2O_2 and $^{\cdot}$OH [19]. It has been proposed that H_2O_2 is formed by a dismutation of $O_2^{\cdot-}$ known to occur either spontaneously or catalyzed by endogenous superoxide dismutase and the interaction of $O_2^{\cdot-}$ with a PSII metal center [55]. $^{\cdot}$OH is formed in illuminated PSII membranes through the reduction of H_2O_2 via the Fenton reaction [55]. Recently, the production of $^{\cdot}$OH has been demonstrated in the presence of either phenolic- or urea-type herbicides [42].

However, the major mechanism of $O_2^{\cdot-}$ production in chloroplasts is that O_2 is reduced by ferredoxin and the electron acceptor of PSI [18,21]. In addition, highly reduced photosynthetic electron carriers would enhance reduction of O_2 by PSI, resulting in subsequent formation of $O_2^{\cdot-}$, H_2O_2 and $^{\cdot}$OH [20,54,58]. Based on fast Chl fluorescence (Fig. 1A and Table 1), it is showed that TeA inhibits the reduction of end acceptors on the PSI acceptor side which is the action target of paraquat. As a result, it deviates electrons from the PSI acceptor side to reduce O_2 generating $O_2^{\cdot-}$ and its decomposition product H_2O_2 [18]. Taking into consideration the fact that the concentration of 250 μM TeA used is about the concentration required to block PSII electron transport activity by 50% [9] and does not block the forward electron flow completely (Fig. 2A, Table 1), hence it is proposed that the production of TeA-induced $O_2^{\cdot-}$ on the level of PSII should be small compared to that at PSI.

Tentoxin from *A. alternata* inhibits chloroplast ATPase activity, causing blockage of the dissipation of the electrochemical proton gradient and thylakoid overenergization, resulting in $O_2^{\cdot-}$ and H_2O_2 generation in chloroplasts [59]. So, this might be another important source of ROS production in chloroplasts since TeA significantly inhibited the activity of chloroplast ATPase (Fig. 2B). The liner electron flow storing redox free energy through PSII, PSI, ferredoxin, and finally NADPH is coupled to the transthylakoid proton gradient, which is maintained by ATP-hydrolysis in the dark [53,60]. Thus, overreduction

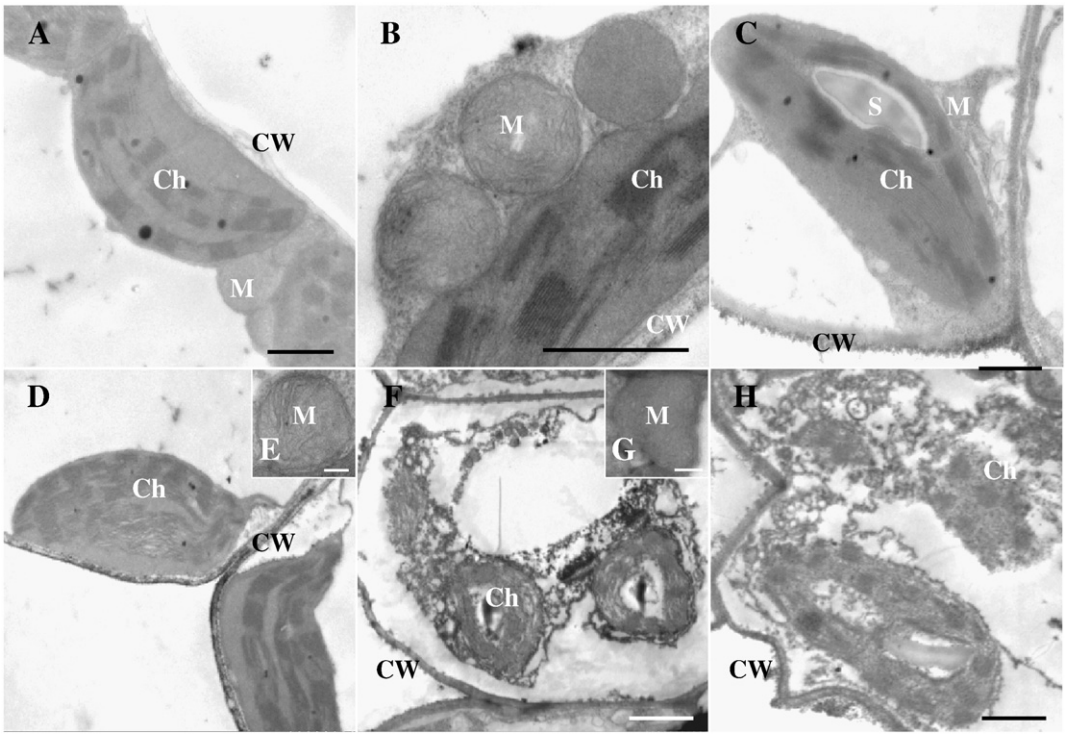

Fig. 9. Ultrastructural changes in mesophyll cells of *E. adenophorum* during TeA-induced cell death. Epidermis-less leaf segments were induced in 1% methanol (control) for 12 h or 250 μM TeA for 4, 5, 6, 9 and 12 h under illumination. Experiments were repeated three times with similar results. (A) No change in ultrastructure was observed in control sample cells. (B) Chloroplast and mitochondrion and other organelles remained normal structurally intact after 4 h of TeA treatment. (C) Evident plasmolysis shown in TeA-treated mesophyll cells at 5 h. Note that chloroplast remained structurally intact. (D) Disorganized grana lamellae and distorted shape of chloroplast and plasmolysis shown in mesophyll cells at 6 h. Note that mitochondrion kept intact (E). (F) Grana lamellae disintegration and chloroplast envelope disruption and mitochondrion distortion change (G) observed in mesophyll cells after 9 h of TeA treatment. Note that cell wall kept normal. (H) By 12 h, TeA-treated mesophyll cells showed significant organelle degradation. Note that chloroplast formed vesicles and cytoderm turned to be distorted or ruptured. CW, cell wall; Ch, chloroplast; M, mitochondrion; S, starch. (A–C) Bar = 1 μm; (D, F, H) bar = 2 μm; (E, G) bar = 200 nm.

of Q_A in PSII and a distinct decrease of ATP-hydrolysis would lead to thylakoid overenergization, allowing the formation of ^{3}Chl, which in turn can react with O_2 to form $^1O_2$ and generate other toxic ROS [40].

Taken together, TeA-induced the generation not only of $^1O_2$ but also of $O_2^{\cdot-}$ as well as H_2O_2 and $^{\cdot}OH$ in chloroplasts. This is a corporate result of multiple effect on PSII electron transport, chloroplast ATPase activity, the energization level in thylakoids, and even PSI electron acceptor side.

4.2. Oxidative damage produced by chloroplastic oxidative burst results in cell death

ROS is one of the main causes for injury, and death in plants under environmental stress [61]. Especially $^{\cdot}OH$ and $^1O_2$, are highly reactive and can produce irreversible oxidative injury to cells [11,62]. The highest toxic radicals $^{\cdot}OH$ directly attack most biomolecules in living cells. This can cause the damage of the site-specific points on account of the very short life of $^{\cdot}OH$, so that cells and organelles "leak", leading to irreparable metabolic dysfunction and cell death, and eventually to rapid leaf wilting and desiccation [21,63,64]. H_2O_2 is thought to be an important signaling molecule leading to changes in gene expression [65]. Nevertheless, for a cell, the main risk produced by H_2O_2 and $O_2^{\cdot-}$ comes from the generation of $^{\cdot}OH$ radicals [66]. $^1O_2$ is more reactive than H_2O_2 and $O_2^{\cdot-}$, which can even diffuse out of the chloroplast into cytosol [67]. It can also react directly with proteins, pigments, lipids and many biomolecules. It can disrupt cell membranes, subsequently causing chloroplast swelling and membrane leakage, and ultimately cellular destruction and plant necrosis. As a result, the formation of other ROS could be stimulated, which would cause further severe damaging effects on cells [68]. In addition, several reports have pronounced that $^1O_2$ as a signal can activate several stress-response pathways [69], and induce cryptochrome-dependent cell death in *Arabidopsis thaliana* [70].

During TeA treatment, chloroplast-derived ROS involved not only highly active $^{\cdot}OH$ and $^1O_2$ but also H_2O_2 and $O_2^{\cdot-}$. These ROS reacted with a variety of cellular components and caused in mesophyll cells severe injury through chlorophyll breakdown, membrane integrity destruction, lipid peroxidation and organelle degradation (Figs. 8 and 9). Furthermore, these oxidative damages take place very quickly, within several hours following the beginning of the challenge, which can be suppressed by ROS scavengers because ROS generation is an earlier event than the injury of mesophyll cells.

According to prior reports, PSII herbicides cause cell and tissue necrosis through oxidative damage caused by herbicide-induced chloroplastic $^1O_2$ generation. One route is that chlorosis is a result of photo-oxidation, caused by chlorophyll and carotenoids destruction, due to excess energy. Another route for necrosis, is through inhibition of electron transport, converts excess energy to oxygen and forms $^1O_2$ which destroys membrane lipids, causing leakage of cell contents, finally resulting in desiccation of the plant tissue [21,67]. Obviously, TeA-triggered leaf tissue necrosis is the latter, where the action sites of TeA are not chlorophylls and carotenes [71]. It is clear as shown that TeA treatment induced $O_2^{\cdot-}$ and highly active $^{\cdot}OH$ in mesophyll cells. Bipyridinium herbicides (e.g. paraquat and diquat) cause cell necrosis and kill plants with extremely high rate constants attributed to the production of $O_2^{\cdot-}$ and highly active $^{\cdot}OH$ [21,58]. Hence, the mechanism of TeA-caused oxidative burst and damage also exhibits similarities to that caused by bipyridinium herbicides, even though TeA proved to be a PSII inhibitor.

As a fungal toxin, TeA might also share some characteristics of other phytotoxins during toxin-plant interaction. Many pathogenic toxins e.g. victorin [13,72–75], AAL-toxin [16,36], FB1 [76,77] etc. can

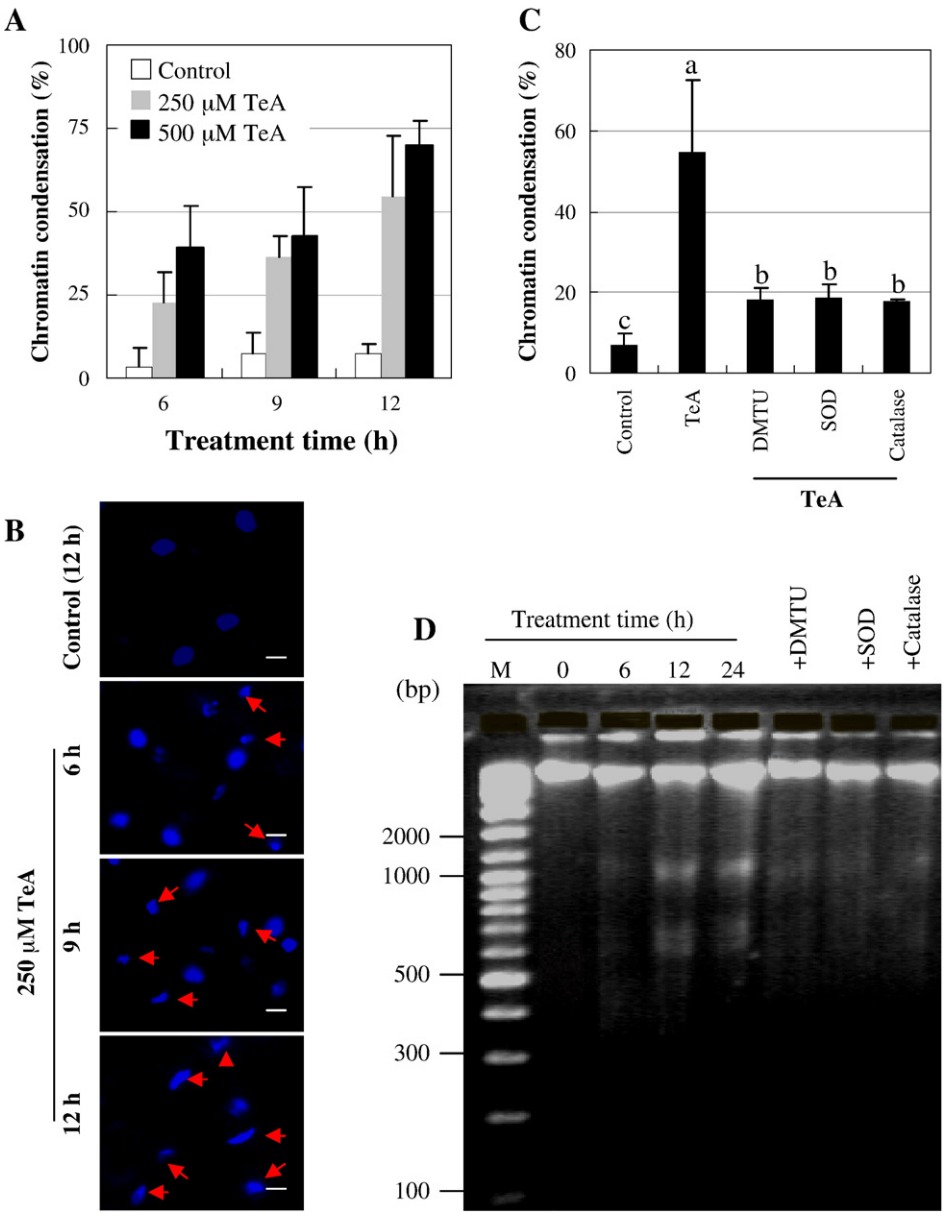

Fig. 10. Effect of TeA-treated mesophyll cells on nuclear chromatin and DNA. Epidermis-less leaf segments of *E. adenophorum* were treated with 1% methanol (control), 250 or 500 μM TeA for the indicated times under illumination. For prevention of TeA-induced chromatin condensation and DNA fragments, leaf segments were co-incubated with 250 μM TeA and ROS scavengers DMTU (1 mM) or SOD (400 U/ml) or catalase (300 U/ml) for 12 h. (A) Frequency of chromatin condensation of mesophyll cells after TeA treatment. (B) Nuclear chromatin condensation of 250 μM TeA-treated mesophyll cells at the indicated time points. (C) Effect of ROS scavengers on nuclear chromatin condensation. At least three hundred mesophyll cell nuclei were counted. Red arrows indicate condensed nuclei. The criteria for chromatin condensation based on the size of nuclei were founded to quantify TeA-induced condensed nuclei, which was less than the half size of normal nucleus and higher intensity of blue fluorescence. Bar = 10 μm. Data are presented as means ± SD ($n = 5$). Means denoted by the same letter did not significantly differ at $p < 0.05$. (D) TeA-induced DNA fragments and effect of ROS scavengers on the TeA-induced DNA fragments.

induce ROS burst and trigger PCD in host-plants [78]. Recent studies indicated that chloroplast-mediated ROS also play significant roles in the processes of plant PCD systems [41,79–83]. However, our experiments suggested that a visible apoptosis-like cell death does not occur in the process of TeA-induced cell death and leaf necrosis (Fig. 10). In fact, the chloroplastic oxidative burst (Figs. 4–6) occurred prior to cell destruction (Fig. 9), which precedes the chromatin condensation and DNA breakage (Fig. 10) in TeA-treated mesophyll cells. This can be explained that TeA-induced ROS react directly with nuclei and result in chromatin condensation and DNA cleavage. Another possible explanation is that necrotic type cell death may be involved in this damage. This type of cell death is characterized by cytoplasmic swelling, loss of plasma membrane integrity, dilation of cytoplasmic organelles, moderate chromatin condensation and without DNA ladders [84,85]. Investigations with diuron indicated that photo-oxidative damage can result in a necrosis type cell death [86]. At lower diuron concentration, ion leakage and membrane damage seem to result from the activation of the EXECUTER1-dependent necrotic death. At higher concentration, a high $^1O_2$ level is responsible for necrotic death controlled by EXECUTER1 gene.

In conclusion, as a photosynthetic inhibitor that is a fungal phytotoxin, TeA-induced cell destruction and leaf necrosis within a very short time. This is a direct result of oxidative damage through a chloroplast-originated ROS burst. Here, a specific mode of action of TeA is described as follows (Fig. 11): when leaves were treated with TeA, with that PSII electron transport beyond Q_A and the reduction of end acceptors on the PSI acceptor side and chloroplast ATPase activity are inhibited, followed occurrence of charge recombination, electron

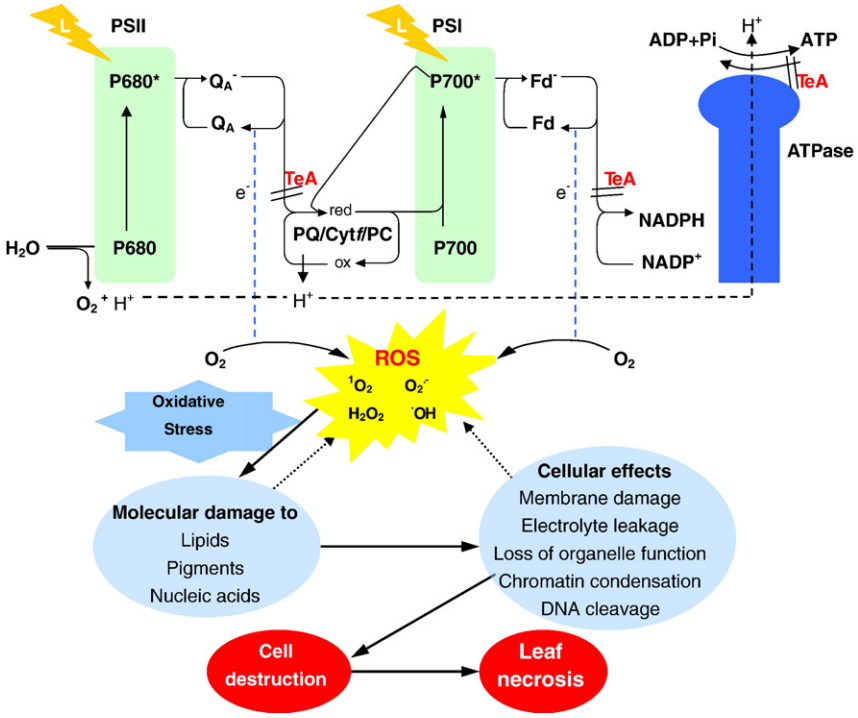

Fig. 11. Suggested model scheme of action of TeA. PSI, photosystem I; PSII, photosystem II; P680, PSII reaction center pigments; P700, PSI reaction center pigments; Q_A, primary quinone acceptors of PSII; PQ, plastoquinone; Cyt *f*, cytochrome *f*; PC, plastocyanin; Fd, ferredoxin; e, electron; H_2O_2, hydrogen peroxide; $O_2^{\cdot-}$, superoxide radicals; $^1O_2$, singlet oxygen; $^{\cdot}OH$, hydroxyl radical; L, light.

leakage to O_2 and thylakoid overenergization, resulting in the chloroplast-derived ROS eruption. An excess of ROS attacks directly pigments, lipids, proteins and DNA, and then causes chlorophyll breakdown, electrolyte leakage, lipid peroxidation, cell membrane disruption, nucleus damage and, subsequently, leads to cell destruction and leaf tissue necrosis and ultimately kills the plants.

Acknowledgements

We are thankful to Prof. Dr. Reto J. Strasser (Geneva University), Dr. J. Lydon (USDA) and Dr. Q.X. Li (Hawaii University) for improvement of the manuscript. Research was supported by China 863 Program (2006AA10A214), Science Foundation of Jiangsu Province (BK2008338), New Teacher Foundation of Doctoral Program of Education Ministry of China (200803071004), Science & Technology Pillar Program of Jiangsu Province (BE2008313), Foundation of Doctoral Program of Education Ministry of China (20090097110018) and 111 Project (B07030).

Appendix A. Supplementary data

Supplementary data associated with this article can be found, in the online version, at doi:10.1016/j.bbabio.2009.12.007.

References

[1] N. Montemurro, A. Visconti, *Alternaria* metabolites—chemical and biological data, in: J. Chelkowski, A. Visconti (Eds.), Alternaria Biology, Plant Diseases and Metabolites, Elsevier Science, Amsterdam, 1992, pp. 449–541.
[2] S. Qiang, Z.X. Wan, Y.F. Dong, Y.H. Li, Phytotoxicity of crude metabolites produced by *Alternaria alternata* to Crofton weed, The sustainable management of weeds meeting the 21st century in China, Guangxi Nationality Press, Nanning, 1999, pp. 158–165.
[3] B.T. Rosett, R.H. Sankhala, C.E. Stickings, M.E.U. Taylor, R. Thomas, Studies in the biochemistry of micro-organisms. Metabolites of *Alternaria tenuis auct*: culture filtrate products, Biochem. J. 67 (1957) 390–400.
[4] N.D. Davies, U.L. Diner, G. Morgan-Jones, Tenuazonic acid production by *Alternaria alternata* and *Alternaria tenuissima* isolated from cotton, Appl. Environ. Microbiol. 34 (1977) 155–157.
[5] M.A. Friedman, V. Aggarwal, G.E. Lester, Inhibition of epidermal DNA synthesis by cycloheximide and other inhibitors of protein synthesis, Res. Commun. Chem. Pathol. Pharmacol. 11 (1975) 311–318.
[6] H. Yuki, K. Kariya, Y. Hashimoto, Synthesis and anti-tumor activity of tenuazonic acid analogues, Chem. Pharm. Bull. 15 (1967) 727–729.
[7] G.L. Gallardo, N.I. Pen, P. Chacana, H.R. Terzolo, G.M. Cabrera, L-Tenuazonic acid, a new inhibitor of *Paenibacillus larva*, World J. Microbiol. Biotechnol. 20 (2004) 609–612.
[8] G. Meazza, B.E. Scheffler, M.R. Tellez, A.M. Rimando, J.G. Romagni, S.O. Duke, D. Nanayakkara, I.A. Khan, E.A. Abourashed, F.E. Dayan, The inhibitory activity of natural products on plant p-hydroxyphenylpyruvate dioxygenase, Phytochemistry 59 (2002) 281–288.
[9] S.G. Chen, X.M. Xu, X.B. Dai, C.L. Yang, S. Qiang, Identification of tenuazonic acid as a novel type of natural photosystem II inhibitor binding in Q_B-site of *Chlamydomonas reinhardtii*, Biochim. Biophys. Acta 1767 (2007) 306–318.
[10] S.G. Chen, C.Y. Yin, X.B. Dai, S. Qiang, X.M. Xu, Action of tenuazonic acid, a natural phytotoxin, on photosystem II of spinach, Environ. Exp. Bot. 62 (2008) 279–289.
[11] K. Apel, H. Hirt, Reactive oxygen species: metabolism, oxidative stress, and signal transduction, Annu. Rev. Plant Biol. 55 (2004) 373–399.
[12] I.M. Moller, P.E. Jensen, A. Hansson, Oxidative modifications to cellular components in plants, Annu. Rev. Plant Biol. 58 (2007) 459–481.
[13] N. Yao, Y. Tada, M. Sakamoto, H. Nakayashiki, P. Park, Y. Tosa, S. Mayama, Mitochondrial oxidative burst involved in apoptotic response in oats, Plant J. 30 (2002) 567–579.
[14] L.V. Bindschedler, J. Dewdney, K.A. Blee, J.M. Stone, T. Asai, J. Plotnikov, C. Denoux, T. Hayes, C. Gerrish, D.R. Davies, F.M. Ausubel, G.P. Bolwell, Peroxidase-dependent apoplastic oxidative burst in *Arabidopsis* required for pathogen resistance, Plant J. 47 (2006) 851–863.
[15] T. Shinogi, T. Suzuki, Y. Narusaka, P. Park, Ultrastructural localization of hydrogen peroxide in host leaves treated with AK-toxin I produced by *Alternaria alternata* Japanese pear pathotype, J. Gen. Plant Pathol. 68 (2002) 38–45.
[16] T.S. Gechev, I.Z. Gadjiev, J. Hille, An extensive microarray analysis of AAL-toxin-induced cell death in *Arabidopsis thaliana* brings new insights into the complexity of programmed cell death in plants, Cell. Mol. Life Sci. 61 (2004) 1185–1197.
[17] J.D. Williamson, J.G. Scandalios, Differential response of maize catalases and superoxide dismutases to the photoactivated fungal toxin cercosporin, Plant J. 2 (1992) 351–358.
[18] B. Hock, E.F. Elstner, Plant Toxicology, 4th edn.Marcel Dekker Press, New York, 2005.
[19] K. Asada, Production and scavenging of reactive oxygen species in chloroplasts and their functions, Plant Physiol. 141 (2006) 391–396.
[20] C. Laloi, K. Apel, A. Danon, Reactive oxygen signaling: the latest news, Curr. Opin. Plant Biol. 7 (2004) 323–328.

[21] B. Halliwell, Oxygen radicals: their formation in plant tissues and their role in herbicide damage, in: N.R. Baker, M.P. Percival (Eds.), Herbicides, Elsevier Science, Amsterdam, 1991, pp. 87–129.
[22] N. Yao, Y. Tada, P. Park, H. Nakayashiki, Y. Tosa, S. Mayama, Novel evidence for apoptotic cell response and differential signals in chromatin condensation and DNA cleavage in victorin-treated oats, Plant J. 28 (2001) 13–26.
[23] J.H. Joo, S.Y. Wang, J.G. Chen, A.M. Jones, N.V. Fedoroff, Different signaling and cell death roles of heterotrimeric G protein α and β subunits in the *Arabidopsis* oxidative stress responsed to ozone, Plant Cell 17 (2005) 957–970.
[24] R.J. Strasser, M. Tsimilli-Michael, A. Srivastava, Analysis of the chlorophyll a fluorescence transient, in: G.C. Papageorgiou, Govindjee (Eds.), Chlorophyll a Fluorescence: a Signature of Photosynthesis, Springer Press, Netherlands, 2004, pp. 321–362.
[25] P.A. Jursinic, Flash polarographic detection of superoxide production as a means of monitoring electron flow between photosystems I and II, FEBS Lett. 90 (1978) 15–20.
[26] G.E. Anthon, A.T. Jagendorf, Effect of methanol on spinach thylakoid ATPase, Biochim. Biophys. Acta 723 (1983) 358–365.
[27] N. Shimizu, N. Hosogi, G.S. Hyon, S. Jiang, K. Inoue, P. Park, Reactive oxygen species (ROS) generation and ROS-induced lipid peroxidation are associated with plasma membrane modifications in host cells in response to AK-toxin I from *Alternaria alternata* Japanese pear pathotype, J. Gen. Plant Pathol. 72 (2006) 6–15.
[28] M. Orozco-Cardenas, C.A. Ryan, Hydrogen peroxide is generated systemically in plant leaves by wounding and systemin via the octadecanoid pathway, Proc. Natl. Acad. Sci. USA 96 (1999) 6553–6557.
[29] J.A. Hernández, M.A. Ferrer, A. Jiménez, A.R. Barceló, F. Sevilla, Antioxidant systems and $O_2^{\cdot-}/H_2O_2$ production in the apoplast of pea leaves. Its relation with salt-induced necrotic in minor veins, Plant Physiol. 127 (2001) 817–831.
[30] A. Allan, R. Fluhr, Two distinct sources of elicited reactive oxygen species in tobacco epidermal cells, Plant Cell 9 (1997) 1559–1572.
[31] S. Abel, A. Theologis, Transient transformation of *Arabidopsis* leaf protoplasts: a versatile experimental system to study gene expression, Plant J. 5 (1994) 421–427.
[32] D.A. Berthold, G.T. Babcock, C.F. Yocum, A highly resolved, oxygen evolving photosystem II preparation from the spinach thylakiod membranes: EPR and electron-transport properties, FEBS Lett. 134 (1981) 231–234.
[33] K. Liu, J. Sun, Y.G. Song, B. Liu, Y.K. Xu, S.X. Zhang, Q. Tian, Y. Liu, Superoxide, hydrogen peroxide and hydroxyl radical in D1/D2/cytochrome *b*-559 photosystem II reaction center complex, Photosynth. Res. 81 (2004) 41–47.
[34] E. Hideg, C. Spetea, I. Vass, Singlet oxygen production in thylakoid membranes during photoinhibition as detected by EPR spectroscopy, Photosynth. Res. 39 (1994) 191–199.
[35] C.S. Bestwick, I.R. Brown, M.H.R. Bennett, J.W. Mansfield, Localization of hydrogen peroxide accumulation during the hypersensitive reaction of lettuce cells to *Pseudomonas syringae* pv *phaseolicola*, Plant Cell 9 (1997) 209–221.
[36] H. Wang, J. Li, R.M. Bostock, D.G. Gilchrist, Apoptosis: a functional paradigm for programmed plant cell death induced by a host-selective phytotoxin and invoked during development, Plant Cell 8 (1996) 375–391.
[37] R.J. Strasser, A. Srivastava, Govindjee, Polyphasic chlorophyll a fluorescence transient in plants and cyanobateria, Photochem. Photobiol. 61 (1995) 32–42.
[38] X.G. Zhu, Govindjee, N.R. Baker, Chlorophyll a fluorescence induction kinetics in leaves predicted from a model describing each discrete step of excitation energy and electron transfer associated with photosystem II, Planta 223 (2005) 114–133.
[39] G. Schansker, S.Z. Tóth, R.J. Strasser, Methylviolegen and dibromothymoquinone treatments of pea leaves reveal the role of photosystem I in the Chl *a* fluorescence rise OJIP, Biochim. Biophys. Acta 1706 (2005) 250–261.
[40] A. Kanazawa, D.M. Kramer, In vivo modulation of nonphotochemical exciton quenching (NPQ) by regulation of the chloroplast ATP synthase, Proc. Natl. Acad. Sci. USA 99 (2002) 12789–12794.
[41] L.E. Bakeeva, E.V. Dzyubinskaya, V.D. Samuilov, Programmed death in plants: ultrastructural changes in pea guard cells, Biochemistry (Moscow) 70 (2005) 972–979.
[42] C. Fufezan, A.W. Rutherford, A. Krieger-Liszkay, Singlet oxygen production in herbicide-treated photosystem II, FEBS Lett. 532 (2002) 407–410.
[43] A.W. Rutherford, A. Krieger-Liszkay, Herbicide-induced oxidative stress in photosystem II, Trends Biochem. Sci. 26 (2001) 648–653.
[44] G. Ananyev, G. Renger, U. Wacker, V. Klimov, The photoproduction of superoxide radicals and the superoxide dismutase activity of PSII: the possible involvement of cytochrome *b*559, Photosynth. Res. 41 (1994) 327–338.
[45] B. Demming-Adams, W.W. Adams, Xanthophyll cycle and light stress in nature, Planta 198 (1996) 460–470.
[46] M.D. Jacobson, Reactive oxygen species and programmed cell death, Trends Biochem. Sci. 21 (1996) 83–86.
[47] R. Mittler, Oxidative stress, antioxidants and stress tolerance, Trends Plant Sci. 7 (2002) 405–410.
[48] S.M.P. Khurana, S.K. Pandey, D. Sarkar, A. Chanemougasoundharam, Apoptosis in plant disease response: a close encounter of the pathogen kind, Curr. Sci. India 88 (2005) 740–752.
[49] B. Halliwell, J.M.C. Gutteridge, Oxygen toxicity, oxygen radicals, transition metals and disease, Biochem. J. 219 (1984) 1–14.
[50] G. Britton, P. Barry, A.J. Young, Carotenoids and chlorophylls: herbicidal inhibition of pigment biosynthesis, in: A.D. Dodge (Ed.), Herbicides and Plant Metabolism, Cambridge University Press, New York, 1989, pp. 51–72.
[51] F.E. Dayan, S.O. Duke, Herbicides: protoporphyrinogen oxidase inhibitors, in: J.R. Plimmer, D.W. Gammon, N.N. Ragsdale, T. Roberts (Eds.), Encyclopedia of Agrochemicals, John Wiley & Sons, New York, NY, 2003, pp. 850–863.
[52] A. Krieger-Liszkay, C. Fufezan, A. Trebst, Singlet oxygen production in photosystem II and related protection mechanism, Photosynth. Res. 98 (2008) 551–564.
[53] A. Krieger-Liszkay, Singlet oxygen production in photosynthesis, J. Exp. Bot. 56 (2005) 337–346.
[54] B. Förster, C.B. Osmond, B.J. Pogson, Improved survival of very high light and oxidative stress is conferred by spontaneous gain-of-function mutations in Chlamydomonas, Biochim. Biophys. Acta 1709 (2005) 45–57.
[55] P. Pospíšil, Production of reactive oxygen species by photosystem II, Biochim. Biophys. Acta 1787 (2009) 1151–1160.
[56] R.E. Cleland, S.C. Grace, Voltammetric detection of superoxide production by photosystem II, FEBS Lett. 457 (1999) 348–352.
[57] S.P. Zhang, J. Weng, J.X. Pan, T.Z. Tu, S. Yao, C.H. Xu, Study on the photo-generation of superoxide radicals in Photosystem II with EPR spin trapping techniques, Photosynth. Res. 75 (2003) 41–48.
[58] C.F. Babbs, J.A. Pham, R.C. Coolbaugh, Lethal hydroxyl radical production in paraquat-treated plants, Plant Physiol. 90 (1989) 1267–1270.
[59] N. Holland, Y. Evron, M.A.K. Jansen, M. Edelman, U. Pick, Involvement of thylakoid overenergization in tentoxin-induced chlorosis in *Nicotiana* spp, Plant Physiol. 114 (1997) 887–892.
[60] T.J. Avenson, J.A. Cruz, D.M. Kramer, Modulation of energy-dependent quenching of excitons in antennae of higher plants, Proc. Natl. Acad. Sci. USA 101 (2004) 5530–5535.
[61] R. Grene, Oxidative stress and acclimation mechanisms in plants, in: C.R. Somerville, E.M. Meyerowitz (Eds.), American Society of Plant Biologists, The Arabidopsis Book, Rockville MD, 2002, doi:10.1199/tab.0036.1, available at: http://www.aspb.org/publications/arabidopsis/.
[62] S. Munné-Bosch, T. Jubany-Marí, L. Alegre, Drought-induced senescence is characterized by a loss of antioxidant defences in chloroplast, Plant Cell Environ. 24 (2001) 1319–1327.
[63] M.V. Beligni, L. Lamattina, Nitric oxide protects against cellular damage produced by methylviologen herbicides in potato plants, Nitric Oxide Biol. Chem. 3 (1999) 199–208.
[64] F.D. Hess, Light-dependent herbicides: an overview, Weed Sci. 48 (2000) 160–170.
[65] S.J. Neill, R. Desikan, J. Hancock, Hydrogen peroxide signaling, Curr. Opin. Plant Biol. 5 (2002) 388–395.
[66] J.F. Palatnik, E.M. Valle, N. Carrillo, Oxidative stress and damage in chloroplasts from dawn to dusk, in: A. Hemantaranjan (Ed.), Advances in Plant Physiology, vol. 4, Scientific Publishers (India), Jodhpur, 2002, pp. 75–88.
[67] A. Krieger-Liszkay, A. Trebst, Tocopherol is the scavenger of singlet oxygen produced by triplet states of chlorophyll in the PSII reaction centre, J. Exp. Bot. 57 (2006) 1677–1684.
[68] J.R. Anthony, K.L. Warczak, T.J. Donohue, A transcriptional response to singlet oxygen, a toxic byproduct of photosynthesis, Proc. Natl. Acad. Sci. USA 102 (2005) 6502–6507.
[69] R.G.L. op den Camp, D. Przybyla, C. Ochsenhein, C. Laloi, C. Kim, A. Danon, D. Wagner, É. Hideg, C. Göbel, I. Feussner, M. Nater, K. Apel, Rapid induction of distinct stress responses after the release of singlet oxygen in *Arabidopsis*, Plant Cell 15 (2003) 2320–2332.
[70] A. Danon, N.S. Coll, K. Apel, Cryptochrome-1-dependent execution of programmed cell death induced by singlet oxygen in *Arabidopsis thaliana*, Proc. Natl. Acad. Sci. USA 103 (2006) 17036–17041.
[71] X.B. Dai, S.G. Chen, S. Qiang, Q.F. An, R.X. Zhang, Effect of toxin from *Alternaria alternata* (Fr.) Keissler on leaf photosynthesis of *Eupatorium adenophorum* Spreng, Acta Phytopathol. Sin. 34 (2004) 55–60.
[72] Y. Tada, S. Hata, Y. Takata, H. Nakayashiki, Y. Tosa, S. Mayama, Induction and signaling of an apoptotic response typified by DNA laddering in the defense response of oats to infection and elicitors, Mol. Plant Microbe Interact. 14 (2001) 477–486.
[73] Y. Tada, K. Kusaka, S. Betsuyaku, T. Shinogi, M. Sakamoto, Y. Ohura, S. Hata, Y. Takata, T. Mori, Y. Tosa, S. Mayama, Victorin triggers programmed cell death and the defense response via interaction with a cell surface mediator, Plant Cell Physiol. 46 (2005) 1787–1798.
[74] N. Yao, S. Imai, Y. Tada, H. Nakayashiki, Y. Tosa, P. Park, S. Mayama, Apoptotic cell death is a common response to pathogen attack in oats, Mol. Plant Microbe Interact. 15 (2002) 1000–1007.
[75] N. Yao, B.J. Eisfelder, J. Marvin, J.T. Greenberg, The mitochondrion—an organelle commonly involved in programmed cell death in *Arabidopsis thaliana*, Plant J. 40 (2004) 596–610.
[76] T. Asai, J.M. Stone, J.E. Heard, Y. Kovtun, P. Yorgey, J. Sheen, F.M. Ausubel, Fumonisin B1-induced cell death in *Arabidopsis* protoplasts requires jasmonate-, ethylene-, and salicylate-dependent signaling pathways, Plant Cell 12 (2000) 1823–1835.
[77] J.M. Stone, J.E. Heard, T. Asai, F.M. Ausubel, Simulation of fungal-mediated cell death by Fumonisin B1 and selection of Fumonisin B1-resistant (fbr) *Arabidopsis* mutants, Plant Cell 12 (2000) 1811–1822.
[78] N.A. Eckardt, Ins and outs of programmed cell death and toxin action, Plant Cell 17 (2005) 2849–2851.
[79] V.D. Samuilov, E.M. Lagunova, E.V. Dzyubinskaya, D.S. Izyumov, D.B. Kiselevsky, Y. V. Makarova, Involvement of chloroplasts in the programmed death of plant cells, Biochemistry (Moscow) 67 (2002) 627–634.
[80] V.D. Samuilov, E.M. Lagunova, S.A. Gostimsky, K.N. Timofeev, M.V. Gusev, Role of chloroplast photosystem II and I in apoptosis of pea guard cells, Biochemistry (Moscow) 68 (2003) 912–917.
[81] V.D. Samuilov, E.M. Lagunova, D.B. Kiselevsky, E.V. Dzyubinskaya, Y.V. Makarova, M.V. Gusev, Role of chloroplast photosystem II and I in apoptosis of pea guard cells, Biosci. Rep. 23 (2003) 103–117.

[82] N. Yao, J.T. Greenberg, *Arabidopsis* ACCELERATED CELL DEATH2 modulates programmed cell death, Plant Cell 18 (2006) 397–411.
[83] P. Mühlenbock, M. Szechyńska-Hebda, M. Plaszczyca, M. Baudo, P.M. Mullineaux, J.E. Parker, B. Karpińska, S. Karpiński, Chloroplast signaling and *LESION SIMULATING DISEASE1* regulate crosstalk between light acclimation and immunity in *Arabidopsis*, Plant Cell 20 (2008) 2339–2356.
[84] G. Kroemer, W.S. El-Deiry, P. Golstein, M. Peter, D. Vaux, P. Vandenabeele, B. Zhivotovsky, M.V. Blagosklonny, W. Malorni, P.A. Knight, M. Piacentini, S. Nagata, G. Melino, Classification of cell death: recommendations of the nomenclature committee on cell death, Cell Death Differ. 12 (2005) 1463–1467.
[85] W.X. Zong, C.B. Thompson, Necrotic death as a cell fate, Genes Dev. 20 (2006) 1–15.
[86] D. Wagner, D. Przybyla, R. op den Camp, C. Kim, F. Landgraf, K.P. Lee, M. Würsch, C. Laloi, M. Nater, E. Hideg, K. Apel, The genetic basis of singlet oxygen-induced stress responses of *Arabidopsis thaliana*, Science 306 (2004) 1183–1185.